

False vacuum decay rates, more precisely

Wen-Yuan Ai,^{*} Jean Alexandre[†] and Sarben Sarkar[‡]

*Theoretical Particle Physics and Cosmology, King's College London,
Strand, London WC2R 2LS, UK*

Abstract

We develop a method for accurately calculating vacuum decay rates beyond the thin-wall regime in pure scalar field theory at the one-loop level of the effective action. It accounts for radiative effects resulting from quantum corrections to the classical bounce, including gradient effects stemming from the inhomogeneity of the bounce background. To achieve this, it is necessary to compute not only the functional determinant of the fluctuation operator in the background of the classical bounce but also its functional derivative evaluated at the classical bounce. The former is efficiently calculated using the Gel'fand-Yaglom method. We illustrate how the latter can also be calculated with the same method, combined with a computation of various Green's functions.

^{*} wenyuan.ai@kcl.ac.uk

[†] jean.alexandre@kcl.ac.uk

[‡] sarben.sarkar@kcl.ac.uk

Contents

1	Introduction	2
2	Callan–Coleman formalism and the tree-level bounce	3
3	Quantum-corrected bounce and radiative corrections to the decay rate	5
4	Functional determinants for an $O(4)$ background and the Gel’fand-Yaglom method	9
5	Functional derivative of a functional determinant	14
6	Numerical example	17
6.1	$B^{(0)}$ and $B^{(1)}$	18
6.2	$B^{(2)}$	20
7	Conclusions	21
A	Solving Green’s functions	24
A.1	$G_l(r, r'; \varphi)$ and $\hat{G}_l(r, r')$	24
A.2	$\mathcal{G}(r, r')$	26
B	Renormalisation with dimensional regularisation	26

1 Introduction

One of the most striking features of the Standard Model (SM) is that the electroweak vacuum is metastable [1–11]. The measured 125 GeV Higgs boson [12, 13], together with the 173 GeV top quark [14], suggests that the Higgs potential in the SM develops a lower minimum due to the renormalisation running of the Higgs self-interaction coupling. The electroweak vacuum could then decay to the true vacuum via tunnelling, which is a first-order phase transition in quantum field theory. State-of-the-art calculations suggest that the electroweak vacuum lies at the edge of the stable region, having a lifetime longer than the present age of the Universe [11, 15–19].¹

In contrast to the running couplings, the radiative corrections to tunneling are computed less accurately. The transition rate is sensitive to a solitonic field configuration in Euclidean space, called the “bounce” [20, 21]. This bounce configuration also encodes the information

¹The scalar potential, the top Yukawa and the electroweak gauge couplings have been extracted from data with full 2-loop next-to-next-leading order (NNLO) precision [15, 16]. These parameters have been extrapolated to large energies with full 3-loop NNLO renormalisation-group-equation (RGE) precision [16].

of the nucleated critical bubble. Typically, the bounce is calculated from the tree-level scalar potential with the running coupling constants evaluated at the scale corresponding to the bounce radius. However, the bounce is an inhomogeneous configuration, and the beta functions for the couplings do not account for the effects of the background inhomogeneity. The inhomogeneity of the bounce requires us to go beyond the effective potential. Such effects from background inhomogeneity, as well as the corresponding higher-loop radiative corrections, have not yet been included in the full SM computations but are only studied in simpler scalar [22–24], Yukawa [25], and gauge [26] theories in the planar thin-wall approximation. These studies are based on a Green’s function method developed earlier in Ref. [27]. See also Refs. [28–30] for the case of two-dimensional spacetime.

We extend previous work by going beyond the thin-wall regime. In order to calculate the quantum-corrected bounce, we need both the functional determinants of the fluctuation operators and their functional derivatives evaluated at the classical bounce (see Eq. (20) or Eq. (30) below). The functional determinants in the $O(4)$ -symmetric backgrounds can be efficiently computed by the Gel’fand-Yaglom method [31, 32]. We show that the functional derivative of a functional determinant can be computed with the same method, combined with a computation of various Green’s functions. This method is closely related to the Green’s function method used in Refs. [22–27]. Our method is applied numerically to compute the corresponding radiative effects in an archetypal scalar model.

The outline of the paper is as follows. In the next section, we briefly review the standard Callan-Coleman formalism for false vacuum decay in terms of the classical bounce. In Sec. 3, we reformulate the decay rate using the one-particle-irreducible (1PI) effective action [33] in a way that radiative corrections to the decay rate can be incorporated. In Sec. 4, we introduce the powerful Gel’fand-Yaglom method for computing functional determinants. In Sec. 5, we show how the Gel’fand-Yaglom method, in combination with a Green’s function method, is used to compute the quantum corrections to the classical bounce and the decay rate. In Sec. 6 we give the results of numerical calculations using our method. In Sec. 7, we give our conclusions. For completeness, some technical details are presented in the appendices. In Appendix A, we give a general introduction to how to solve the Green’s functions. In Appendix B, we discuss how to renormalise the effective one-loop action using the dimensional renormalisation scheme. In the paper, we use $\hbar = c = 1$.

2 Callan–Coleman formalism and the tree-level bounce

We consider the archetypal model,

$$\mathcal{L}_M = \frac{1}{2}\eta^{\mu\nu}(\partial_\mu\Phi)(\partial_\nu\Phi) - U(\Phi), \quad (1)$$

where $\eta^{\mu\nu}$ is the Minkowski metric with signature $\{+, -, -, -\}$ and

$$U(\Phi) = \frac{1}{2}m^2\Phi^2 - \frac{1}{3!}g\Phi^3 + \frac{1}{4!}\lambda\Phi^4. \quad (2)$$

The couplings m^2 , g , λ all take positive values. When $g^2 > 8\lambda m^2/3$, the potential has two local minima. For $8\lambda m^2/3 < g^2 < 3\lambda m^2$, $\varphi = 0^2$ is the global minimum; for $g^2 > 3\lambda m^2$, the global minimum becomes

$$\varphi_{\text{TV}} = \frac{3g + \sqrt{9g^2 - 24\lambda m^2}}{2\lambda}. \quad (3)$$

When $g^2 = 3\lambda m^2$, the two local minima become degenerate. Below we consider the parameter region $g^2 > 3\lambda m^2$. The potential (see Fig. 1) has two minima at $\varphi_{\text{FV}} = 0$ and φ_{TV} , corresponding to the false and true vacua respectively. In the potential, we have chosen $U(\varphi_{\text{FV}}) = 0$ for convenience.

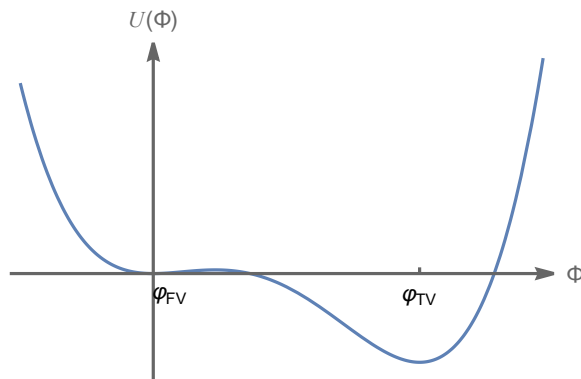


Figure 1: The classical potential $U(\Phi)$ for the archetypical scalar model with false vacuum decay, given by Eqs. (1) and (2).

The decay rate is obtained from the Euclidean transition amplitude

$$Z[0] = \langle \varphi_{\text{FV}} | e^{-H\mathcal{T}} | \varphi_{\text{FV}} \rangle = \int \mathcal{D}\Phi e^{-S[\Phi]}, \quad (4)$$

where H is the Hamiltonian, \mathcal{T} is the amount of Euclidean time taken by the transition and S is the Euclidean action. In terms of $Z[0]$, the decay rate per volume is given by [21]

$$\frac{\gamma}{V} = \lim_{\mathcal{T} \rightarrow \infty} \frac{2}{V\mathcal{T}} |\text{Im}(\ln Z[0])|. \quad (5)$$

The partition function $Z[0]$ is evaluated by using the method of steepest descent for path integrals. The classical equation of motion in Euclidean spacetime reads

$$-\partial^2\varphi + U'(\varphi) = 0, \quad (6)$$

with the boundary conditions $\varphi|_{\tau \rightarrow \pm\infty} = \varphi_{\text{FV}}$ and $\dot{\varphi}|_{\tau=0} = 0$, where the dot denotes the derivative with respect to the Euclidean time τ . A trivial solution is $\varphi(x) = \varphi_{\text{FV}}$. There is a nontrivial

²We use φ to denote the vacuum expectation value of the quantum field Φ , $\varphi = \langle 0 | \Phi | 0 \rangle$. This should be clearer when we introduce the effective action below.

solution—the *bounce*—which is $O(4)$ symmetric in Euclidean spacetime. The bounce solution is relevant for false vacuum decay and describes a field configuration that starts and ends in Euclidean time in the false vacuum. Working in four-dimensional hyperspherical coordinates, the equation of motion reads

$$-\frac{d^2\varphi(r)}{dr^2} - \frac{3}{r} \frac{d\varphi(r)}{dr} + U'(\varphi(r)) = 0, \quad (7)$$

where $r = \sqrt{\tau^2 + \mathbf{x}^2}$. The boundary conditions become $\varphi(r \rightarrow \infty) = \varphi_{\text{FV}}$ and $d\varphi(r)/dr|_{r=0} = 0$. We denote this classical bounce solution as $\varphi_b^{(0)}$.

Aside from the single bounce solution, there are also multi-bounce solutions that go back and forth from the false vacuum N times, for arbitrary N . These multi-bounce configurations exponentiate [21, 34, 35] in analogous to disconnected vacuum Feynman diagrams. Integrating the fluctuations about the stationary points requires one to analyse the eigenfunctions of the fluctuation operators. In particular, the operator $-\partial^2 + U''(\varphi_b^{(0)})$ contains negative and zero modes (see Sec. 4 below). Carefully dealing with some subtleties from these particular modes, one obtains the decay rate per unit volume [21]

$$\frac{\gamma}{V} = \left(\frac{B^{(0)}}{2\pi}\right)^2 \left| \frac{\det'[-\partial^2 + U''(\varphi_b^{(0)})]}{\det[-\partial^2 + U''(\varphi_{\text{FV}})]} \right|^{-1/2} e^{-B^{(0)}}, \quad (8)$$

where $B^{(0)} = S[\varphi_b^{(0)}] - S[\varphi_{\text{FV}}]$, \det' means that the zero eigenvalues are omitted from the determinant and a prefactor $\sqrt{B^{(0)}/2\pi}$ is included for each of the four collective coordinates that are related to the zero modes corresponding to spacetime translations [36]. Using $S[\varphi_{\text{FV}}] = 0$ we have

$$B^{(0)} = 2\pi^2 \int_0^\infty dr r^3 \left[\frac{1}{2} (\partial_r \varphi_b^{(0)}(r))^2 + U(\varphi_b^{(0)}) \right]. \quad (9)$$

3 Quantum-corrected bounce and radiative corrections to the decay rate

We reformulate Eq. (5) such that radiative effects can be systematically considered, using the 1PI effective action [33]. To keep the discussion general, we work in d -dimensional spacetime. But we will return to four-dimensional spacetime later. First, we introduce the partition function in the presence of a source J ,

$$Z[J] = \int \mathcal{D}\Phi e^{-S[\Phi] + \int d^d x J(x)\Phi(x)}. \quad (10)$$

The one-point function in the presence of the source J is given by

$$\varphi_J(x) = \langle 0|\Phi(x)|0\rangle_J = \frac{\delta \ln Z[J]}{\delta J(x)}. \quad (11)$$

The effective action then is defined as the Legendre transform

$$\Gamma[\varphi_J] = -\ln Z[J] + \int d^d x J(x)\varphi_J(x). \quad (12)$$

From the effective action, one obtains the *quantum* equation of motion for the one-point function, $\delta\Gamma[\varphi_J]/\delta\varphi_J(x) = J(x)$. Note that Γ has no explicit dependence on J . Denoting $\varphi \equiv \varphi_{J=0}$, one obtains the equation of motion for the vacuum expectation value in the absence of sources by setting $J = 0$,

$$\frac{\delta\Gamma[\varphi]}{\delta\varphi(x)} = 0. \quad (13)$$

A nontrivial $O(4)$ -symmetric solution to Eq. (13) would give the quantum-corrected bounce φ_b . In terms of the effective action, the decay rate per volume (5) can be written as

$$\frac{\gamma}{V} = \frac{2 |\text{Im} e^{-(\Gamma[\varphi_b] - \Gamma[\varphi_{\text{FV}}])}|}{V\mathcal{T}}. \quad (14)$$

This is the formula used in Refs. [22, 34, 37, 38] where it is implicitly assumed that $\Gamma[\varphi_{\text{FV}}] = 0$. Since adding constant and linear terms in the Lagrangian does not affect the dynamics (when gravity is not considered), in the renormalisation procedure one can always implement $\varphi_{\text{FV}} = 0$ and $\Gamma[\varphi_{\text{FV}}] = 0$, even beyond the tree level.

On denoting the fluctuation operator evaluated at a general configuration φ as

$$\mathcal{M}[\varphi] = -\partial^2 + U''(\varphi), \quad (15)$$

the one-loop effective action reads

$$\Gamma^{(1)}[\varphi] = S[\varphi] + \frac{1}{2} \ln \frac{\det \mathcal{M}[\varphi]}{\det \widehat{\mathcal{M}}} \equiv S[\varphi] + \frac{1}{2} D[\varphi], \quad (16)$$

where $\widehat{\mathcal{M}} \equiv \mathcal{M}[\varphi_{\text{FV}}]$ and $D[\varphi] \equiv \ln \frac{\det \mathcal{M}[\varphi]}{\det \widehat{\mathcal{M}}}$. Above, the normalisation choice $\Gamma[\varphi_{\text{FV}}] = 0$ is made.

The bounce at the one loop, $\varphi_b^{(1)}$, satisfies

$$\left. \frac{\delta S[\varphi]}{\delta\varphi(x)} \right|_{\varphi_b^{(1)}} + \frac{1}{2} \left. \frac{\delta D[\varphi]}{\delta\varphi(x)} \right|_{\varphi_b^{(1)}} = 0. \quad (17)$$

Expanding this equation about $\varphi_b^{(0)} \equiv \varphi_b^{(1)} - \Delta\varphi_b$ gives³

$$[-\partial^2 + U''(\varphi_b^{(0)})]\Delta\varphi_b + \frac{1}{2} \left. \frac{\delta D[\varphi]}{\delta\varphi(x)} \right|_{\varphi_b^{(0)}} = 0, \quad (18)$$

³We assume that the one-loop corrected bounce is close to the classical bounce. If the false vacuum is generated by radiative corrections in the first place, it is necessary to use the two-particle irreducible effective action [39] as explained in Refs. [37, 38].

where a crossed wheel denotes the classical bounce $\varphi_b^{(0)}$. Note that this two-loop diagram is obtained from the expansion $\varphi_b^{(1)} = \varphi_b^{(0)} + \Delta\varphi_b$ of the *one-loop* diagram on using $G(x, y; \varphi_b^{(1)})$ as the propagator. When using $G(x, y; \varphi_b^{(0)})$ as the propagator, we say that the last term in Eq. (20) corresponds to a *partial* two-loop corrections, but not to full two-loop corrections.

Making use of $O(d)$ -symmetry. Although $D[\varphi]$ and also the effective action are functionals of general configurations $\varphi(x)$, it is assumed that the corrected bounce remains $O(d)$ -symmetric. For this reason, it is sufficient to obtain $D[\varphi]$ for $O(d)$ -symmetric configurations $\varphi(r)$ and take the functional derivative of the former with respect to the latter. In this case, we can treat $\varphi(r)$ as a one-dimensional function and derive its equation of motion by directly varying the action $S[\varphi]$ and $D[\varphi]$ with respect to the one-dimensional field $\varphi(r)$. To illustrate this, we first consider the classical equation of motion for the bounce, (7) generalised to d -dimensional spacetime. As explained in Sec. 2, one can derive it from Eq. (6) by assuming $O(d)$ -symmetry. However, one can also derive it by applying the $O(d)$ -symmetry to the classical action

$$S[\varphi] = \frac{2\pi^{d/2}}{\Gamma(d/2)} \int dr r^{d-1} \left[\frac{1}{2} (\partial_r \varphi(r))^2 + U(\varphi(r)) \right], \quad (26)$$

where $\Gamma(x)$ is the Gamma function, and varying it with respect to the one-dimensional field $\varphi(r)$. Similarly, we can do the same procedure for $D[\varphi]$. Then the one-loop equation of motion reads

$$\begin{aligned} \frac{\delta S[\varphi]}{\delta \varphi(r)} \Big|_{\varphi_b^{(1)}} + \frac{1}{2} \frac{\delta D[\varphi]}{\delta \varphi(r)} \Big|_{\varphi_b^{(1)}} &= 0 \\ \Rightarrow \frac{2\pi^{d/2} r^{d-1}}{\Gamma(d/2)} \left[-\frac{d^2}{dr^2} - \frac{d-1}{r} \frac{d}{dr} + U''(\varphi_b^{(0)}) \right] \Delta\varphi_b(r) + \frac{1}{2} \frac{\delta D[\varphi]}{\delta \varphi(r)} \Big|_{\varphi_b^{(0)}} &= 0, \quad (27) \end{aligned}$$

where again we have expanded the functional derivative at the classical bounce and neglected perturbatively small higher-order terms. Note that in this procedure $\delta D[\varphi]/\delta \varphi(r)|_{\varphi_b^{(0)}}$ is not equal to $\delta D[\varphi]/\delta \varphi(x)|_{\varphi_b^{(0)}}$; they even have different mass dimensions due to the different Dirac delta functions generated in the two procedures for taking the functional derivative. The reason for introducing this new procedure is as follows. Below we have explicit expressions of $D[\varphi]$ only for $O(4)$ -symmetric configurations $\varphi(r)$ instead of general four-dimensional configurations $\varphi(x)$. As a consequence, we can take the functional derivative of $D[\varphi]$ only with respect to $\varphi(r)$, rather than with respect to the general four-dimensional function $\varphi(x)$. Even when one assumes $O(d)$ -symmetry for the one-point function, one still integrates over all possible fluctuations about $\varphi(r)$ in deriving the expression of $D[\varphi]$, as indicated by the sum over l in Eqs. (45), (46) below.

From Eq. (27),

$$\Delta\varphi_b(r) = -\frac{1}{2} \int dr' \mathcal{G}(r, r') \left[\frac{\Gamma(d/2)}{2\pi^{d/2} r^{d-1}} \frac{\delta D[\varphi]}{\delta \varphi(r')} \Big|_{\varphi_b^{(0)}} \right], \quad (28)$$

where $\mathcal{G}(r, r')$ is the Green's function, satisfying

$$\left[-\frac{d^2}{dr^2} - \frac{d-1}{r} \frac{d}{dr} + U''(\varphi_b^{(0)}) \right] \mathcal{G}(r, r') = \delta(r - r'). \quad (29)$$

This procedure finally gives

$$\Gamma^{(1)}[\varphi_b^{(1)}] = S[\varphi_b^{(0)}] + \frac{1}{2} D[\varphi_b^{(0)}] + \frac{1}{4} \int dr \frac{\delta D[\varphi]}{\delta \varphi(r)} \Big|_{\varphi_b^{(0)}} \Delta \varphi_b(r), \quad (30)$$

where the last term is a one-dimensional integral. Note that the last term above is *not* obtained from the last term in Eq. (20) by simply taking $\varphi(x) = \varphi(r)$. As we commented above, $D[\varphi]/\delta\varphi(r)|_{\varphi_b^{(0)}} \neq \delta D[\varphi]/\delta\varphi(x)|_{\varphi_b^{(0)}}$ and we should have

$$\begin{aligned} \left(\frac{1}{4} \int d^d x \frac{\delta D[\varphi]}{\delta \varphi(x)} \Big|_{\varphi_b^{(0)}} \Delta \varphi_b(x) \right) \Big|_{\varphi(x)=\varphi(r)} &= \frac{1}{4} \int dr \frac{\delta D[\varphi]}{\delta \varphi(r)} \Big|_{\varphi_b^{(0)}} \Delta \varphi_b(r) \\ \Rightarrow \frac{\delta D[\varphi]}{\delta \varphi(r)} \Big|_{\varphi_b^{(0)}} &= \frac{2\pi^{d/2} r^{d-1}}{\Gamma(d/2)} \frac{\delta D[\varphi]}{\delta \varphi(x)} \Big|_{\varphi_b^{(0)}}. \end{aligned} \quad (31)$$

From Eqs. (28) and (30), we see that, at the one-loop level of the effective action, a self-consistent bounce solution and the corrected decay rate are derived from $D[\varphi_b^{(0)}]$ and the functional derivative $\delta D[\varphi]/\delta\varphi(r)|_{\varphi_b^{(0)}}$ (or $\delta D[\varphi]/\delta\varphi(x)|_{\varphi_b^{(0)}}$ if one uses Eqs. (18) and (20)).

In the following, we use the Gel'fand-Yaglom method to compute the functional determinant $D[\varphi]$ as well as its functional derivative.

4 Functional determinants for an $O(4)$ background and the Gel'fand-Yaglom method

The powerful Gel'fand-Yaglom method [31] is widely employed in calculations for tunneling in theoretical as well as phenomenological studies, see e.g. Refs. [7, 18, 19, 32, 40–42]. It is used in BubbleDet [43], a recent Python package that aims to compute functional determinants.

For a general $O(d)$ -symmetric configuration φ that approaches zero (the false vacuum φ_{FV}) for $r \rightarrow \infty$, we have the decomposition

$$D[\varphi] = \sum_{l=0}^{\infty} \text{deg}(l; d) \ln \left(\frac{\det \mathcal{M}_l[\varphi]}{\det \widehat{\mathcal{M}}_l} \right), \quad (32)$$

where⁵

$$\mathcal{M}_l[\varphi] = -\frac{d^2}{dr^2} - \frac{d-1}{r} \frac{d}{dr} + \frac{l(l+d-2)}{r^2} + U''(\varphi(r)), \quad (33a)$$

$$\widehat{\mathcal{M}}_l = -\frac{d^2}{dr^2} - \frac{d-1}{r} \frac{d}{dr} + \frac{l(l+d-2)}{r^2} + m^2, \quad (33b)$$

and

$$\text{deg}(l; d) = \frac{(d+2l-2)\Gamma(d+l-2)}{\Gamma(l+1)\Gamma(d-1)}. \quad (34)$$

For each l , one can calculate the functional determinant ratio using the Gel'fand-Yaglom theorem [31]. Define the functions $\psi_l(r)$ and $\hat{\psi}_l(r)$ as the solutions to the following equations

$$\mathcal{M}_l[\varphi]\psi_l(r; \varphi) = 0, \quad \widehat{\mathcal{M}}_l\hat{\psi}_l(r) = 0, \quad (35)$$

with the same leading regular behavior at $r = 0$. The Gel'fand-Yaglom theorem states that

$$\frac{\det \mathcal{M}_l[\varphi]}{\det \widehat{\mathcal{M}}_l} = \frac{\psi_l(\infty; \varphi)}{\hat{\psi}_l(\infty)} \equiv T_l(\infty; \varphi). \quad (36)$$

First, we show an asymptotic analysis for $\hat{\psi}_l(r)$ and $\psi_l(r)$. For $r \rightarrow 0$, one can ignore the potential term in the operators $\widehat{\mathcal{M}}_l$ and $\mathcal{M}_l[\varphi]$. Therefore, the solutions regular at $r = 0$ are proportional to r^l . Without loss of generality, both $\hat{\psi}_l(r)$ and $\psi_l(r)$ are normalised to r^l as $r \rightarrow 0$. Then we obtain

$$\hat{\psi}_l(r) = \left(\frac{2}{m}\right)^{l+d/2-1} \Gamma\left(l + \frac{d}{2}\right) r^{1-d/2} I_{l+d/2-1}(mr). \quad (37)$$

$I_{l+d/2-1}(x)$ are the modified Bessel functions of the first kind, satisfying

$$\left[-\frac{d^2}{dr^2} - \frac{1}{r} \frac{d}{dr} - \left(m^2 + \frac{(l+d/2-1)^2}{r^2} \right) \right] I_{l+d/2-1}(mr) = 0. \quad (38)$$

$I_{l+d/2-1}(mr) \sim r^{l+d/2-1} (m/2)^{l+d/2-1} / \Gamma(l+d/2)$ for $r \rightarrow 0$. Substituting $\psi_l = T_l \hat{\psi}_l$ into Eq. (35), one obtains

$$\left[-\frac{d^2}{dr^2} - \left(2m \frac{I_{l+d/2-2}(mr)}{I_{l+d/2-1}(mr)} - \frac{2l+d-3}{r} \right) \frac{d}{dr} + W(\varphi(r)) \right] T_l(r; \varphi) = 0, \quad (39)$$

where

$$W(\varphi) = U''(\varphi) - m^2. \quad (40)$$

⁵The operators $\mathcal{M}_l[\varphi]$ are obtained when substituting $\Psi(r, \theta) = \psi_l(r)Y_l(\theta)$ (where $Y_l(\theta)$ are the hyperspherical harmonics) into the eigenequations for $\mathcal{M}[\varphi]$. It is the same for $\widehat{\mathcal{M}}_l$.

The boundary conditions are

$$T_l(0; \varphi) = 1, \quad \left. \frac{dT_l(r; \varphi)}{dr} \right|_{r=0} = 0. \quad (41)$$

We note that Eq. (39) can be written in a slightly different form due to the recursion relations of the modified Bessel functions.

In the following, we take $d = 4$.

Divergences and renormalisation

The sum

$$\sum_{l=0}^{\infty} (l+1)^2 \ln T_l(\infty; \varphi) \quad (42)$$

is divergent. This is not surprising because we are calculating the one-loop effective action whose divergence can only be removed by counterterms. Formally, we can write the renormalised one-loop effective action as

$$S_1^{\text{ren}}[\varphi] = S_0[\varphi] + \Delta S[\varphi] + S_{\text{ct}}[\varphi], \quad (43)$$

where $S_0[\varphi]$ is the classical action, $\Delta S[\varphi] = D[\varphi]/2$, and $S_{\text{ct}}[\varphi]$ is the contribution from the counterterms. In the renormalised effective action, all the couplings (including mass parameters) are now renormalised ones. The details of the counterterms and renormalised couplings depend on the renormalisation scheme.. In the $\overline{\text{MS}}$ scheme, we have

$$S_1^{\text{ren}}[\varphi] = S_0^{\overline{\text{MS}}}[\varphi] + (\Delta S[\varphi] - (\Delta S[\varphi])^{\text{pole}}) \equiv S_0^{\overline{\text{MS}}}[\varphi] + (\Delta S[\varphi])^{\text{reg}}, \quad (44)$$

where $S_0^{\overline{\text{MS}}}$ is the lowest-order action expressed in terms of the renormalised $\overline{\text{MS}}$ couplings, and $(\Delta S[\varphi])^{\text{pole}}$ is the pole of the divergent part of ΔS defined according to the $\overline{\text{MS}}$ renormalisation prescription.

In the literature, two slightly different methods of obtaining a $(\Delta S[\varphi])^{\text{reg}}$ are used. The first was used by Dunne and Min [40] (see also [44, 45]), and followed by Refs. [41–43]. The second one was used even earlier by Baacke and Kiselev [46], and followed in Refs. [7, 19, 47, 48]. Below, we shall show that when the functional derivative with respect to φ is taken, the first method gives a UV divergent result. This means that the first method is at most valid only “on shell”, i.e., only for the classical bounce solution but not for variations about it. The second method still gives a UV-convergent functional derivative. However, we observe that the regularised one-loop functional determinant contains a UV-finite tadpole term (linear term in φ) for our model, which would shift the position of the false vacuum from zero. For self-consistency, we therefore propose removing such a non-vanishing tadpole by a linear counterterm. This would modify one of the finite terms ($A_{\text{fin}}^{(1)}$) to be discussed below.

Before we write down the explicit expressions for $(\Delta S[\varphi])^{\text{reg}}$, we discuss why there are two different points of view on the divergence in Eq. (42). The first one is that the divergence is caused by the large l behaviour of $\ln T_l(\infty; \varphi)$ and one needs to derive the analytical expression of $\ln T_l(\infty; \varphi)$ as a series of l . This can be done by the WKB method for solving Eq. (39) for large l [40, 43]. Then one can use the dimensional regularisation to subtract the pole terms in the sum. This leads to the Dunne-Min formula given below. The second point of view is that the divergence is caused by $W(\varphi) \neq 0$, i.e., by a nonvanishing interaction term. If $W(\varphi) = 0$, then the sum automatically gives zero. In this case, one expands $\ln T_l(\infty; \varphi)$ in powers of W . The divergence is found to be contained in the terms of order $\mathcal{O}(W)$, $\mathcal{O}(W^2)$ (each as a sum over l). These terms however correspond to the standard UV divergences of the effective action and thus can be expressed by loop integrals. (The inhomogeneity of the background field becomes irrelevant in the deep UV.) Once again, one can obtain pole terms in the loop integrals by dimensional regularisation which will be then subtracted from the sum. For more details see Appendix B. This procedure leads to the Baacke-Kiselev formula, Eq. (46).

The first method gives [40, 44]

$$\begin{aligned} (\Delta S[\varphi])_{\text{DM}}^{\text{reg}} &= \frac{1}{2} \sum_{l=0}^{\infty} (l+1)^2 \left\{ \ln T_l(\infty; \varphi) - \frac{\int_0^{\infty} dr r W(\varphi)}{2(l+1)} + \frac{\int_0^{\infty} dr r^3 W(\varphi)(W(\varphi) + 2m^2)}{8(l+1)^3} \right\} \\ &- \frac{1}{16} \int_0^{\infty} dr r^3 W(\varphi) (W(\varphi) + 2m^2) \left[\log\left(\frac{\mu r}{2}\right) + \gamma_E + 1 \right], \end{aligned} \quad (45)$$

where γ_E is Euler's constant, and μ is a renormalisation scale.

The second method gives [47]

$$\begin{aligned} (\Delta S[\varphi])_{\text{BL}}^{\text{reg}} &= \frac{1}{2} \sum_{l=0}^{\infty} (l+1)^2 \left\{ \ln T_l(\infty; \varphi) - h_l^{(1)}(\infty; \varphi) - \left[h_l^{(2)}(\infty; \varphi) - \frac{1}{2} \left(h_l^{(1)}(\infty; \varphi) \right)^2 \right] \right\} \\ &+ \frac{1}{2} \left(A_{\text{fin}}^{(1)}[\varphi] - \frac{1}{2} A_{\text{fin}}^{(2)}[\varphi] \right), \end{aligned} \quad (46)$$

where $h_l^{(1)}$, $h_l^{(2)}$ satisfy

$$\left[-\frac{d^2}{dr^2} - \left(2m \frac{I_l(mr)}{I_{l+1}(mr)} - \frac{2l+1}{r} \right) \frac{d}{dr} \right] h_l^{(1)}(r; \varphi) + W(\varphi) = 0, \quad (47a)$$

$$\left[-\frac{d^2}{dr^2} - \left(2m \frac{I_l(mr)}{I_{l+1}(mr)} - \frac{2l+1}{r} \right) \frac{d}{dr} \right] h_l^{(2)}(r; \varphi) + W(\varphi) h_l^{(1)}(r; \varphi) = 0, \quad (47b)$$

with boundary conditions $h_l^{(1,2)}(0; \varphi) = 0$, $dh_l^{(1,2)}(r; \varphi)/dr|_{r=0} = 0$, and

$$A_{\text{fin}}^{(1)}[\varphi] = -\frac{m^2}{8} \left[1 + \ln \left(\frac{\mu^2}{m^2} \right) \right] \int_0^\infty dr r^3 W(\varphi(r)), \quad (48a)$$

$$A_{\text{fin}}^{(2)}[\varphi] = \frac{1}{8} \ln \left(\frac{\mu^2}{m^2} \right) \int dr r^3 [W(\varphi(r))]^2 + \frac{1}{16\pi^2} \int \frac{d^4 k}{(2\pi)^4} |\widetilde{W}(k)|^2 \left[2 - \frac{\sqrt{k^2 + 4m^2}}{|k|} \ln \left(\frac{\sqrt{k^2 + 4m^2} + |k|}{\sqrt{k^2 + 4m^2} - |k|} \right) \right], \quad (48b)$$

where

$$\widetilde{W}(k) = \int d^4 x e^{ikx} W(\varphi(x)). \quad (49)$$

In Appendix B, we derive the above equations. Since $\varphi(x)$ depends on $r = |x|$ only, we can write

$$\widetilde{W}(k) = \frac{4\pi^2}{|k|} \int_0^\infty dr r^2 W(\varphi(r)) J_1(|k|r) \equiv \widetilde{W}(|k|), \quad (50)$$

where J_1 is the Bessel function of the first kind, defined as

$$J_1(|k|r) = \frac{|k|r}{\pi} \int_0^\pi d\theta \sin^2 \theta e^{i|k|r \cos \theta}. \quad (51)$$

We observe that $A_{\text{fin}}^{(1)}$ contains a linear term in φ for our model since $W(\varphi) = -g\varphi + \lambda\varphi^2/2$. As a consequence,

$$\frac{\delta A_{\text{fin}}^{(1)}[\varphi]}{\delta \varphi(r)} = -\frac{m^2}{8} \left[1 + \ln \left(\frac{\mu^2}{m^2} \right) \right] r^3 U'''(\varphi(r)) = \left[1 + \ln \left(\frac{\mu^2}{m^2} \right) \right] \left(\frac{m^2 g}{8} r^3 - \frac{m^2 \lambda}{8} r^3 \varphi(r) \right), \quad (52)$$

is not zero even for $\varphi = 0$. This means that the position of the false vacuum would be shifted if there are no other linear terms in Eq. (46). We show below that such additional linear terms are absent. To be self-consistent, we have to add a linear counterterm to remove the observed tadpole term by requiring

$$\left. \frac{\delta S_1^{\text{ren}}[\varphi]}{\delta \varphi(x)} \right|_{\varphi=0} = 0. \quad (53)$$

This is achieved by simply doing the following replacement,

$$A_{\text{fin}}^{(1)}[\varphi] \rightarrow \overline{A_{\text{fin}}^{(1)}}[\varphi] = -\frac{m^2}{8} \left[1 + \ln \left(\frac{\mu^2}{m^2} \right) \right] \int_0^\infty dr r^3 \overline{W(\varphi(r))}, \quad (54)$$

where an overline means the subtraction of tadpole terms.

For false vacuum decay, it is natural to take $\mu = m$ (as we will do in the following) so that $\overline{A_{\text{fin}}^{(1)}}[\varphi]$ and $A_{\text{fin}}^{(2)}[\varphi]$ simplify further.

One can numerically solve Eq. (47a) to obtain $h_l^{(1)}(r; \varphi)$ (and hence $h_l^{(1)}(\infty; \varphi)$), while $h_l^{(2)}(\infty; \varphi)$ as well as its functional derivative with respect to φ can be computed via a Green's function method with known $h_l^{(1)}(r; \varphi)$, see below.

Zero and negative modes

When taking $\varphi = \varphi_b^{(0)}$, there are four zero modes in the sector $l = 1$. The integral over the fluctuations in the zero-mode directions can be traded for an integral over the collective coordinates of the bounce, giving [43, 44]

$$e^{-\frac{1}{2}(1+1)^2 \ln T_1(\infty; \varphi_b^{(0)})} \rightarrow \underbrace{(V\mathcal{T}) \left(\frac{S_E[\varphi_b^{(0)}]}{2\pi} \right)^2}_{\text{zero-mode contribution}} \left(\frac{\det' \mathcal{M}_1[\varphi_b^{(0)}]}{\det \widehat{\mathcal{M}}_1} \right)^{-2} = (V\mathcal{T}) \left[2\pi A |\partial_r^2 \varphi_b^{(0)}(0)| \right]^2, \quad (55)$$

where A is defined by the normalisation of the asymptotic large r behavior of the classical bounce: $\varphi_b^{(0)}(r) \sim Ar^{-1}K_1(r)$. Here $K_1(r)$ is the modified Bessel function of the second kind. Using the equation of motion for $\varphi_b^{(0)}$, Eq. (7), one has

$$\left. \frac{d^2 \varphi_b^{(0)}(r)}{dr^2} \right|_{r=0} = \frac{U'(\varphi_b^{(0)}(0))}{4}, \quad (56)$$

where we have used $\partial_r \varphi_b^{(0)}(r)/r \rightarrow \partial_r^2 \varphi_b^{(0)}(r)$ as $r \rightarrow 0$. So, formally, we have the replacement

$$\ln T_1(\infty; \varphi_b^{(0)}) \rightarrow -\frac{1}{2} \ln(V\mathcal{T}) - \frac{1}{2} \ln \left[(\pi A U'(\varphi_b^{(0)}(0))/2)^2 \right]. \quad (57)$$

Note that the factor of $V\mathcal{T}$ in Eq. (55) will be cancelled by the same factor in γ/V (cf. Eq. (14)), leading to a finite decay rate per volume.

The lowest eigenvalue mode in the $l = 0$ sector is a negative mode and is responsible for the instability of the false vacuum. Naively, the negative mode leads to divergence in the Gaussian functional integral about the bounce. However, this divergence is simply due to an improper application of the method of steepest descent [21, 32, 49]. With a suitable deformation of the contour into the complex plane whose real axis is generated by the negative mode, one actually obtains the following replacement

$$T_0(\infty; \varphi_b^{(0)}) \rightarrow \left(\pm \frac{i}{2} \right)^{-2} \left| T_0(\infty; \varphi_b^{(0)}) \right|, \quad (58)$$

where the additional factor is due to the contour deformation and gives rise to an imaginary part of the effective action with a particular factor of $1/2$. The sign depends on the direction in which one deforms the contour into the complex plane. Usually, one chooses the way that leads to a positive decay rate. But in our formula (14), we have taken the absolute value, and the sign in Eq. (58) does not matter.

In the following, we show how to take the functional derivative in Eqs. (45) and (46).

5 Functional derivative of a functional determinant

To compute the quantum corrections to the bounce as well as the corresponding corrections to the decay rate, we still need to compute $\delta D[\varphi]/\delta\varphi(r)|_{\varphi_b^{(0)}}$ (cf. Eqs. (28) and (30)). We will use

Eq. (46), which leads

$$\frac{\delta(\Delta S[\varphi])_{\text{BL}}^{\text{reg}}}{\delta\varphi(r)} = \frac{1}{2} \sum_{l=0}^{\infty} (l+1)^2 \left\{ \frac{1}{T_l(\infty; \varphi)} \frac{\delta T_l(\infty; \varphi)}{\delta\varphi(r)} - \frac{\delta h_l^{(1)}(\infty; \varphi)}{\delta\varphi(r)} - \frac{\delta h_l^{(2)}(\infty; \varphi)}{\delta\varphi(r)} + h_l^{(1)}(\infty; \varphi) \frac{\delta h_l^{(1)}(\infty; \varphi)}{\delta\varphi(r)} \right\} + \frac{1}{2} \frac{\delta \overline{A_{\text{fin}}^{(1)}}(\varphi)}{\delta\varphi(r)} - \frac{1}{4} \frac{\delta A_{\text{fin}}^{(1)}(\varphi)}{\delta\varphi(r)}. \quad (59)$$

At the end of this section, we shall comment on the problem if one uses Eq. (45).

We need to compute $\delta T_l(\infty; \varphi)/\delta\varphi$, $\delta h_l^{(1,2)}(\infty; \varphi)/\delta\varphi$. To simplify the notation, we define

$$\mathcal{H}_l[\varphi] \equiv \frac{d^2}{dr^2} + \left(2m \frac{I_l(mr)}{I_{l+1}(mr)} - \frac{2l+1}{r} \right) \frac{d}{dr} - W(\varphi(r)), \quad (60a)$$

$$\widehat{\mathcal{H}}_l \equiv \frac{d^2}{dr^2} + \left(2m \frac{I_l(mr)}{I_{l+1}(mr)} - \frac{2l+1}{r} \right) \frac{d}{dr}. \quad (60b)$$

Then

$$\mathcal{H}_l[\varphi] T_l(r; \varphi) = 0, \quad \widehat{\mathcal{H}}_l h_l^{(1)}(r; \varphi) = W(\varphi(r)), \quad \widehat{\mathcal{H}}_l h_l^{(2)}(r; \varphi) = W(\varphi(r)) h_l^{(1)}(r; \varphi). \quad (61)$$

Taking the functional derivative of the first equation with respect to $\varphi(r)$ gives

$$\mathcal{H}_l[r'; \varphi] \frac{\delta T_l(r'; \varphi)}{\delta\varphi(r)} = - \frac{\delta \mathcal{H}_l[r'; \varphi]}{\delta\varphi(r)} T_l(r'; \varphi) = \delta(r' - r) U'''(\varphi(r')) T_l(r'; \varphi). \quad (62)$$

Viewing r as a fixed number, the above equation in the coordinate r' can then be solved by the Green's function method and we obtain

$$\frac{\delta T_l(r'; \varphi)}{\delta\varphi(r)} = \int dr'' G_l(r', r''; \varphi) \delta(r'' - r) U'''(\varphi(r'')) T_l(r''; \varphi) = G_l(r', r; \varphi) U'''(\varphi(r)) T_l(r; \varphi), \quad (63)$$

where $G_l(r, r'; \varphi)$ satisfies

$$\mathcal{H}_l[\varphi(r)] G_l(r, r'; \varphi) = \delta(r - r'), \quad (64)$$

with the boundary conditions⁶

$$G_l(0, r'; \varphi) = 0, \quad \partial_r G_l(r, r'; \varphi)|_{r=0} = 0. \quad (65)$$

⁶To see these are the correct boundary conditions, one can analyse the equation $\mathcal{H}_l[\varphi + \delta\varphi] T_l(r; \varphi + \delta\varphi) = 0$ by writing $T_l(r; \varphi + \delta\varphi) = T_l(r; \varphi) + \delta T_l(r; \varphi)$. Since $T_l(r; \varphi)$ and $T_l(r; \varphi + \delta\varphi)$ satisfy the same boundary conditions imposed in the Gel'fand-Yaglom theorem, $\delta T_l(r; \varphi)$ has the boundary conditions $\delta T_l(0; \varphi) = 0$, $d\delta T_l(r; \varphi)/dr|_{r=0} = 0$ which are shared by $\delta T_l(r; \varphi)/\delta\varphi$ and thus the Green's function G_l .

Taking $r' = \infty$ one obtains

$$\frac{\delta T_l(\infty; \varphi)}{\delta \varphi(r)} = G_l(\infty, r; \varphi) U'''(\varphi(r)) T_l(r; \varphi). \quad (66)$$

One can apply a similar analysis for the second and third equations in (61). But it is more straightforward to take the functional derivative with explicit expressions of $h_l^{(1,2)}(\infty; \varphi)$. In this case, we need to solve the Green's function

$$\widehat{\mathcal{H}}_l \widehat{G}_l(r, r') = \delta(r - r'), \quad (67)$$

with the same boundary conditions as in Eq. (65). Then

$$h_l^{(l)}(\infty; \varphi) = \int dr' \widehat{G}_l(\infty, r') W(\varphi(r')), \quad (68a)$$

$$h_l^{(2)}(\infty; \varphi) = \int dr' \widehat{G}_l(\infty, r') W(\varphi(r')) h_l^{(1)}(r'; \varphi). \quad (68b)$$

The same expressions are valid if one replaces ∞ with r above. Taking the functional derivative of these expressions, one obtains

$$\frac{\delta h_l^{(1)}(\infty; \varphi)}{\delta \varphi(r)} = \widehat{G}_l(\infty, r) U'''(\varphi(r)), \quad (69a)$$

$$\begin{aligned} \frac{\delta h_l^{(2)}(\infty; \varphi)}{\delta \varphi(r)} &= \widehat{G}_l(\infty, r) U'''(\varphi(r)) h_l^{(1)}(r; \varphi) \\ &+ \int dr' \widehat{G}_l(\infty, r') W(\varphi(r')) \widehat{G}_l(r', r) U'''(\varphi(r)). \end{aligned} \quad (69b)$$

$\widehat{G}_l(r, r')$ can be obtained analytically (see Appendix A) and reads

$$\widehat{G}_l(r, r') = \theta(r - r') \frac{r' I_{l+1}(mr')}{I_{l+1}(mr)} [I_{l+1}(mr) K_{l+1}(mr') - I_{l+1}(mr') K_{l+1}(mr)], \quad (70)$$

where $K_{l+1}(x)$ is the modified Bessel function of the second kind. The Green's functions $G_l(r, r'; \varphi)$ depend on φ and can only be obtained numerically.

From Appendix A, we can see

$$G_l(r, \infty; \varphi) = \widehat{G}_l(r, \infty) = 0. \quad (71)$$

Therefore, one immediately has

$$\left. \frac{\delta T_l(\infty; \varphi)}{\delta \varphi(r)} \right|_{r=\infty} = 0. \quad (72)$$

If one uses Eq. (45), one would obtain a divergent *and cutoff-dependent* result from the second and third terms in the sum over l at $r = \infty$. Therefore, Eq. (45) cannot give a meaningful result

once the functional derivative with respect to $\varphi(r)$ is taken. On the contrary, Eq. (46) gives a finite result because we also have

$$\left. \frac{\delta h_l^{(1)}(\infty; \varphi)}{\delta \varphi(r)} \right|_{r=\infty} = \left. \frac{\delta h_l^{(2)}(\infty; \varphi)}{\delta \varphi(r)} \right|_{r=\infty} = 0, \quad (73)$$

due to the properties in Eq. (71). This also shows that there is no additional tadpole term in the sum over l in Eq. (46), otherwise one would obtain a term proportional to r^3 in the functional derivative, which is not vanishing for $r \rightarrow \infty$.

At last, the functional derivatives of $A_{\text{fin}}^{(1)}[\varphi]$ and $A_{\text{fin}}^{(2)}[\varphi]$ with respect to $\varphi(r)$ read

$$\frac{\delta \overline{A_{\text{fin}}^{(1)}}[\varphi]}{\delta \varphi(r)} = -\frac{m^2 \lambda}{8} r^3 \varphi(r), \quad (74a)$$

$$\begin{aligned} \frac{\delta A_{\text{fin}}^{(2)}[\varphi]}{\delta \varphi(r)} &= \frac{r^2}{16\pi^2} U'''(\varphi(r)) \int d|k| |k|^2 J_1(|k|r) \widetilde{W}(|k|) \\ &\times \left[2 - \frac{\sqrt{|k|^2 + 4m^2}}{|k|} \ln \left(\frac{\sqrt{|k|^2 + 4m^2} + |k|}{\sqrt{|k|^2 + 4m^2} - |k|} \right) \right], \end{aligned} \quad (74b)$$

where $\widetilde{W}(|k|)$ is defined in Eq. (50).

6 Numerical example

With the analysis given in the previous sections, here we discuss the procedure for numerical calculations and provide a numerical example. We leave a more delicate phenomenological study for future work.

Denoting

$$\frac{1}{2} D[\varphi_b^{(0)}] = B^{(1)} - \ln \left(\pm \frac{i}{2} \right) - \ln(V\mathcal{T}), \quad B^{(2)} = \frac{1}{4} \int dr \left. \frac{\delta D[\varphi]}{\delta \varphi(r)} \right|_{\varphi_b^{(0)}} \Delta \varphi_b(r), \quad (75)$$

we can write the decay rate per unit volume as

$$\frac{\gamma}{V} = \frac{2 \text{Im} e^{-\Gamma[\varphi_b^{(1)}]}}{V\mathcal{T}} = e^{-B^{(0)} - B^{(1)} - B^{(2)}}. \quad (76)$$

Recall that $D[\varphi]/2 = \Delta S[\varphi]$. Both here and below, $D[\varphi]$ is regularised even though the superscript “reg” is suppressed. We use the Baacke-Kiselev formula for the regularised one-loop functional determinant (cf. Eq. (46)) with the modification (54).

In the numerical calculations, all the parameters that have mass dimension one take values in the unit of m so that $m = 1$. As a benchmark point, we choose

$$g = 0.66, \quad \lambda = 0.1.$$

The profile of the potential is shown in Fig. 1.

6.1 $B^{(0)}$ and $B^{(1)}$

For convenience of later discussion, we denote

$$f_l[\varphi] \equiv \ln T_l(\infty; \varphi) - h_l^{(1)}(\infty; \varphi) - \left[h_l^{(2)}(\infty; \varphi) - \frac{1}{2} \left(h_l^{(1)}(\infty; \varphi) \right)^2 \right]. \quad (77)$$

Then we have

$$B^{(1)} = \underbrace{\frac{1}{2} \ln |T_0(\infty; \varphi_b^{(0)})|}_{\text{negative-mode replacement (58)}} - \underbrace{\ln \left[(\pi A U'(\varphi_b^{(0)}(0))/2)^2 \right]}_{\text{zero-mode replacement (57)}} + \underbrace{\frac{1}{2} \sum_{l \geq 2} (l+1)^2 f_l[\varphi_b^{(0)}]}_{\text{positive-definite modes (46)}} - \underbrace{\frac{1}{2} \sum_{l=0,1} \left[h_l^{(1)}(\infty; \varphi_b^{(0)}) + h_l^{(2)}(\infty; \varphi_b^{(0)}) - \frac{1}{2} \left(h_l^{(1)}(\infty; \varphi_b^{(0)}) \right)^2 \right] + \frac{1}{2} \left(\overline{A_{\text{fin}}^{(1)}}[\varphi_b^{(0)}] - \frac{1}{2} A_{\text{fin}}^{(2)}[\varphi_b^{(0)}] \right)}_{\text{remaining contribution generated from renormalisation, cf. Eq. (46), (54)}}. \quad (78)$$

We summarise the procedure of computing the bounce and decay rate at the level of the Callan-Coleman formula.

- Step 1: Solve the classical EoM (7) and obtain the classical bounce $\varphi_b^{(0)}$. Substitute it into Eq. (9) to obtain the classical bounce action $B^{(0)}$.
- Step 2: Substitute $\varphi_b^{(0)}$ into Eq. (39) to obtain $T_l(r; \varphi_b^{(0)})$, in particular its limiting value at $r \rightarrow \infty$, $T_l(\infty; \varphi_b^{(0)})$.
- Step 3: Substituting $\hat{G}_l(\infty, r')$ (cf. Eq. (70)) and $\varphi_b^{(0)}$ into Eq. (68a) to obtain $h_l^{(1)}(r; \varphi_b^{(0)})$ and $h_l^{(1)}(\infty; \varphi_b^{(0)})$. Substituting $h_l^{(1)}(r; \varphi_b^{(0)})$ into Eq. (68b), one obtains $h_l^{(2)}(\infty; \varphi_b^{(0)})$.

The zero and negative modes in computing $T_l(\infty; \varphi_b^{(0)})$ need to be properly dealt with as discussed in Sec. 4. With these three steps, one can obtain $B^{(0)}$ and $B^{(1)}$ and thus the Callan-Coleman decay rate.

The classical bounce is obtained via a shooting algorithm and is shown in Fig. 2. The classical bounce action is $B^{(0)} = 12942.7$.

For $B^{(1)}$, we first compute $f_l[\varphi_b^{(0)}]$ for $l \geq 2$. We find that $l_{\text{max}} = 50$ is already a good cutoff. We plot $f_l[\varphi_b^{(0)}]$ in Fig. 3 where we compare the numerical result with $-50/l^4$. Clearly $|f_l[\varphi_b^{(0)}]|$ drops as fast as or faster than $1/l^4$, ensuring a convergent result for the sum in Eq. (78). We obtain

$$\frac{1}{2} \sum_{l \geq 2} (l+1)^2 f_l[\varphi_b^{(0)}] = -10.981. \quad (79)$$

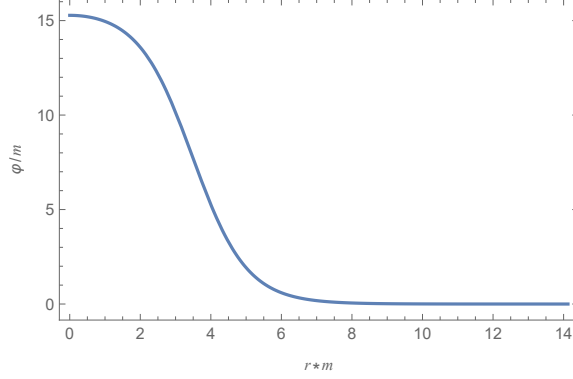


Figure 2: The profile of the classical bounce $\varphi_b^{(0)}(r)$.

For the contribution from $l = 0, 1$, we find

$$B^{(1)} \supset \frac{1}{2} \ln \left| T_0(\infty; \varphi_b^{(0)}) \right| = -1.449, \quad (80a)$$

$$B^{(1)} \supset -\ln \left[(\pi A U'(\varphi_b^{(0)}(0))/2)^2 \right] = -7.388, \quad (80b)$$

$$B^{(1)} \supset -\frac{1}{2} \sum_{l=0,1} \left[h_l^{(1)}(\infty; \varphi_b^{(0)}) + h_l^{(2)}(\infty; \varphi_b^{(0)}) - \frac{1}{2} \left(h_l^{(1)}(\infty; \varphi_b^{(0)}) \right)^2 \right] = -4.671. \quad (80c)$$

Finally, $\overline{A_{\text{fin}}^{(1)}}[\varphi_b^{(0)}]$ and $A_{\text{fin}}^{(2)}[\varphi_b^{(0)}]$ are obtained as

$$\overline{A_{\text{fin}}^{(1)}}[\varphi_b^{(0)}] = -15.177, \quad A_{\text{fin}}^{(2)}[\varphi_b^{(0)}] = -5.322 \quad \Rightarrow \quad \frac{1}{2} \left(\overline{A_{\text{fin}}^{(1)}}[\varphi_b^{(0)}] - \frac{1}{2} A_{\text{fin}}^{(2)}[\varphi_b^{(0)}] \right) = -6.258. \quad (81)$$

In total, we have $B^{(1)} = -30.747$.

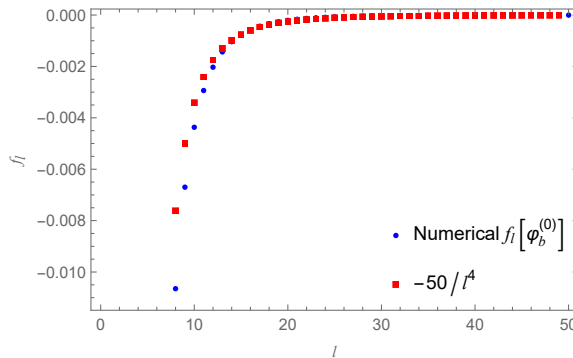


Figure 3: The behavior of f_l as a function of l .

6.2 $B^{(2)}$

To obtain the quantum-corrected bounce and the decay rate at the full one-loop level of the effective action, we need to calculate $\delta D[\varphi]/\delta\varphi(r)|_{\varphi_b^{(0)}}$ (using Eq. (59)) and $\Delta\varphi_b(r)$ (using Eq. (28)). The last two terms in Eq. (59) are trivial because we have their analytical expressions (cf. Eqs. (74)). The remaining calculation requires the following three further steps.

- Step 4: Substituting $\varphi_b^{(0)}$ into Eq. (64), one can obtain $G_l(\infty, r'; \varphi_b^{(0)})$. With $G_l(\infty, r'; \varphi_b^{(0)})$ and $T_l(r; \varphi_b^{(0)})$, one obtains $\delta T_l(\infty; \varphi)/\delta\varphi(r)|_{\varphi_b^{(0)}}$ through Eq. (66).

Further, with $\hat{G}_l(r, r')$ and $h_l^{(1)}(r; \varphi_b^{(0)})$, one can obtain $\delta h_l^{(1)}(\infty; \varphi)/\delta\varphi(r)|_{\varphi_b^{(0)}}$ and $\delta h_l^{(2)}(\infty; \varphi)/\delta\varphi(r)|_{\varphi_b^{(0)}}$ through Eqs. (69).

Substituting all of them and Eqs. (74) into Eq. (59), one can finally obtain $\delta D[\varphi]/\delta\varphi(r)|_{\varphi_b^{(0)}}$.

- Step 5: Compute the Green's function in Eq. (29) and substitute the obtained Green's function $\mathcal{G}(r, r')$ and $\delta D[\varphi]/\delta\varphi(r)|_{\varphi_b^{(0)}}$ into Eq. (28) to obtain $\Delta\varphi_b(r)$.
- Step 6: Finally, substitute the obtained $\Delta\varphi_b(r)$ and $\delta D[\varphi]/\delta\varphi(r)|_{\varphi_b^{(0)}}$ into the second equation in (75) to obtain $B^{(2)}$.

Again, in calculating the functional derivatives with respect to φ , the zero and negative modes need special treatment. *Formally*,

$$\frac{\delta D[\varphi]}{\delta\varphi(r)}\Big|_{\varphi_b^{(0)}} = \lim_{\delta\varphi \rightarrow \mathbf{0}} \frac{D[\varphi_b^{(0)} + \delta\varphi] - D[\varphi_b^{(0)}]}{\delta\varphi(r)}, \quad (82)$$

where $\mathbf{0}$ is a function that equals to zero identically. In the above equation, one therefore needs to look into the spectrum for both $-\partial^2 + U''(\varphi_b^{(0)})$ and $-\partial^2 + U''(\varphi_b^{(0)} + \delta\varphi)$. We expect that for an infinitesimal deformation of the classical bounce $\delta\varphi \rightarrow \mathbf{0}$, the operator $-\partial^2 + U''(\varphi_b^{(0)} + \delta\varphi)$ still contains the same number of zero and negative modes. And we assume that Eq. (58) is still valid for φ infinitely close to $\varphi_b^{(0)}$, so that one can obtain $\delta T_0(\infty; \varphi)/\delta\varphi(r)|_{\varphi_b^{(0)}}$ from that replacement.

For the zero mode, it is more subtle because Eq. (57) is expressed in terms of $\varphi_b^{(0)}$ at $r = 0$ and is not a standard functional of $\varphi_b^{(0)}(r)$. One even cannot formally replace $\varphi_b^{(0)}$ with φ and take the functional derivative of the second term in Eq. (57). We thus will neglect the zero-mode contribution to the functional derivative.⁷ However, we have checked that $\delta h_1^{(1,2)}/\delta\varphi(r)|_{\varphi_b^{(0)}}$ are indeed negligible in the final result of $\delta D[\varphi]/\delta\varphi(r)|_{\varphi_b^{(0)}}$. The obtained $\delta D[\varphi]/\delta\varphi|_{\varphi_b^{(0)}}$ is shown in Fig. 4.

Following Step 5, we obtain the correction to the classical bounce $\Delta\varphi_b(r)$ as shown Fig. 5. The profile of $\Delta\varphi_b(r)$ is negligible compared with $\varphi_b^{(0)}(r)$. However, the additional correction to

⁷The most important contribution of the zero modes to $D[\varphi]$ is the term involving the spacetime volume $V\mathcal{T}$. Contribution from this term is cancelled in Eq. (82) and the remaining contribution is expected to be negligible.

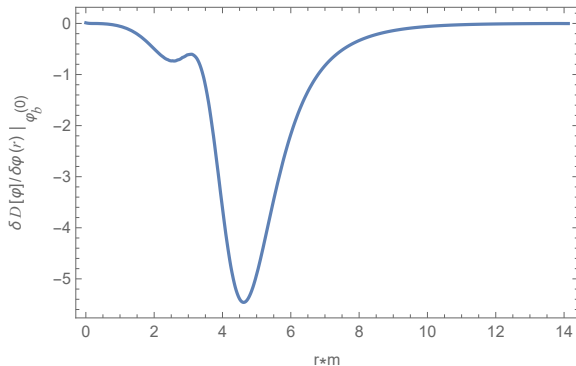


Figure 4: Numerical result for $\delta D[\varphi]/\delta\varphi(r)|_{\varphi_b^{(0)}}$.

the decay rate is obtained as $B^{(2)} = -16.42$ (Step 6), which is 53.4% of $B^{(1)}$. The correction $\Delta\varphi_b(r)$ to the classical bounce is maximal around $rm \simeq 3.5$, which also corresponds to roughly the steepest part of the bubble wall profile. This indicates that these higher-order corrections receive large contributions from the gradients of the bubble wall. This observation is consistent with that made in Ref. [25] for thin-wall bubbles.

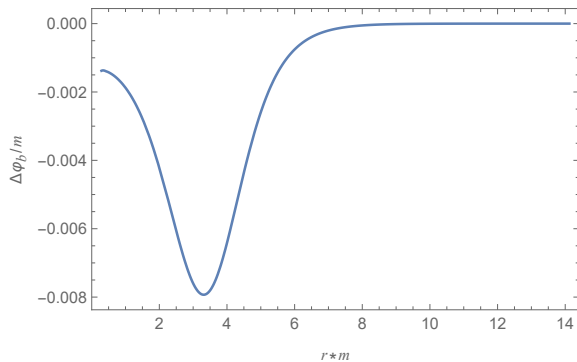


Figure 5: The correction to the classical bounce, $\Delta\varphi(r)$.

7 Conclusions

FVD is a very important phenomenon in quantum field theory and there continue to be many developments both conceptual and methodological [32, 50–67]. In this paper, we propose a systematic procedure to compute the self-consistent bounce solution and its resulting radiative correction to the decay rate at the one-loop level of the effective action. This is achieved by evaluating the one-loop effective action at the one-loop saddle point configuration for the bounce (the self-consistent bounce), instead of the classical one. The method requires the computation of both conventional functional determinants and their functional derivative, both evaluated at the classical bounce. Earlier studies on this are restricted to the thin-wall regime [22, 25, 26] and

are usually based on the “resolvent method” of calculating functional determinants by treating Green’s function as a spectral sum [32, 68–71]. In this work, we have demonstrated that the powerful Gel’fand-Yaglom method can be used to compute both the functional determinants and their functional derivatives, making the computation extremely efficient. In particular, for $O(4)$ -symmetric configurations that asymptotically approach the false vacuum, an explicit expression for the renormalised one-loop effective action in pure scalar field theory is known. We have shown how it is directly used in the computation.

Although the theoretical developments here are general, we provide an explicit numerical study of our archetypal model. Our chosen benchmark point for the mass and coupling parameters is such that the bounce is far away from the thin-wall regime. In this example, the correction $B^{(1)}$ (the decay rate due to the functional determinant evaluated at the classical bounce) is small compared with the classical bounce action $B^{(0)}$. However, the additional correction due to the consideration of the self-consistent bounce, $B^{(2)}$, is of the same order of magnitude (about 50%) as the purely one-loop correction $B^{(1)}$. This indicates that in some precision phenomenological studies when the conventional functional determinants are important, one may be required to consider the self-consistent bounce as well.

Another motivation for considering the self-consistent bounce is to obtain a gauge-independent tunneling rate when gauge fields are involved. It is known that the effective action is gauge-dependent. By the Nielsen identity [34, 72, 73],

$$\left(\xi \frac{\partial \Gamma[\varphi; \xi]}{\partial \xi} + K(\varphi; \xi) \frac{\delta \Gamma[\varphi; \xi]}{\delta \varphi} \right) = 0, \quad (83)$$

where ξ is the gauge parameter, the effective action is only gauge independent at its extrema. Then Eq. (14) gives a gauge-independent decay rate in principle only at the self-consistent bounce [34]. Since the effective action must be truncated, this issue is usually more complicated. For more discussions related to this topic, see Refs. [74–80].

Our method may find applications in physics of the early Universe (see, e.g., Refs. [81–83]), where bubble nucleation can occur at finite temperature [84–88].⁸ At high temperature, the phase transition is dominated by a static, i.e., Euclidean time independent, $O(3)$ -symmetric bounce and the transition rate can be written as [86]

$$\gamma = \frac{\sqrt{|\lambda_-|}}{2\pi} \times 2|\text{Im} \ln Z[\beta]|, \quad (84)$$

where $Z[\beta]$ is the thermal partition function with the temperature $T = 1/\beta$, and λ_- is the negative eigenvalue for the three-dimensional fluctuation operator at the classical bounce. The factor $\sqrt{|\lambda_-|}/(2\pi)$ above may be generalised to include the Langevin damping coefficient [85, 97, 98]. The calculation presented in this paper can be easily generalised to lower-dimensional bounce configurations, e.g., $O(3)$ -symmetric static bounces that are relevant for thermal first-order phase transitions, and therefore can be applied to study radiative corrections in thermal first-order

⁸Gravitational effects could also be very important in some situations [89–96].

phase transitions [99]. However, at finite temperatures, there are many more theoretical uncertainties [100, 101]. The quantum corrections due to the self-consistent bounce might be detectable in experiments involving analogue systems in condensed matter [102–105].

Acknowledgments

The authors of this work are supported by the Engineering and Physical Sciences Research Council (grant No. EP/V002821/1). JA is also supported by the Leverhulme Trust (grant No. RPG-2021-299) and by the Science and Technology Facilities Council (grant No. STFC-ST/X000753/1).

A Solving Green's functions

In this appendix, we outline the procedure on solving Green's functions numerically. Suppose we want to solve the following Green's function

$$L[r]G(r, r') = \delta(r - r'), \quad (\text{A1})$$

where $L[r]$ is a second-order differential operator and $\{r, r'\} \in [0, \infty)$.

A.1 $G_l(r, r'; \varphi)$ and $\hat{G}_l(r, r')$

For $G_l(r, r'; \varphi)$ and $\hat{G}_l(r, r')$, the boundary conditions are of the following type,

$$G(0, r') = 0, \quad \left. \frac{\partial G(r, r')}{\partial r} \right|_{r=0} = 0. \quad (\text{A2})$$

Assume that $\{f_1(r), f_2(r)\}$ are two independent (numerical) solutions to the equation $L[r]f(r) = 0$. Then the Green's function can be written as

$$G(r, r') = \theta(r - r')[A_1^>(r')f_1(r) + A_2^>(r')f_2(r)] + \theta(r' - r)[A_1^<(r')f_1(r) + A_2^<(r')f_2(r)], \quad (\text{A3})$$

where $A_1^{\gtrless}(r')$ and $A_2^{\gtrless}(r')$ shall be determined by the boundary conditions and matching conditions.

The matching conditions are from the following two requirements on $G(r, r')$: (i) $G(r, r')$ is continuous at $r = r'$ when viewed as a function of r ; (ii) $\partial_r G(r, r')$ has a finite jump discontinuity at $r = r'$. The sign and magnitude of this jump depends on the coefficient of the second-derivative term in the operator $L[r]$. We will assume that this coefficient is 1 to be consistent with the operators $\mathcal{H}_l[\varphi]$ and $\hat{\mathcal{H}}_l$. Thus we have

$$[A_1^>(r')f_1(r') + A_2^>(r')f_2(r')] - [A_1^<(r')f_1(r') + A_2^<(r')f_2(r')] = 0, \quad (\text{A4a})$$

$$[A_1^>(r')f_1'(r') + A_2^>(r')f_2'(r')] - [A_1^<(r')f_1'(r') + A_2^<(r')f_2'(r')] = 1. \quad (\text{A4b})$$

After some algebra, one obtains

$$A_1^>(r') - A_1^<(r') = -\frac{f_2(r')}{\mathcal{W}[f_1(r'), f_2(r)]}, \quad (\text{A5a})$$

$$A_2^>(r') - A_2^<(r') = \frac{f_1(r')}{\mathcal{W}[f_1(r'), f_2(r)]}, \quad (\text{A5b})$$

where

$$\mathcal{W}[f_1(r), f_2(r)] = f_1(r)f_2'(r) - f_1'(r)f_2(r) \quad (\text{A6})$$

is the Wronskian.

The functions f_1 and f_2 can be determined by the boundary conditions. We can choose, for example,⁹

$$f_1(0) = 1, f_1'(r)|_{r=0} = 0; \quad f_2(r)|_{r \rightarrow \infty} \rightarrow 0, f_2'(r)|_{r \rightarrow \infty} \rightarrow 0. \quad (\text{A7})$$

In general, the boundary conditions for $f_2(r)$ lead to $f_2(0) \neq 0, f_2'(r)|_{r=0} \neq 0$. Then the boundary conditions for $G(r, r')$ require

$$A_2^<(r') = 0, \quad A_1^<(r') = 0. \quad (\text{A8})$$

Substituting the above into Eqs. (A5), one obtains $A_1^>(r')$ and $A_2^>(r')$ and thus also the Green's function

$$G(r, r') = \theta(r - r') \left[-\frac{f_1(r)f_2(r')}{\mathcal{W}[f_1(r'), f_2(r')]} + \frac{f_1(r')f_2(r)}{\mathcal{W}[f_1(r'), f_2(r')]} \right]. \quad (\text{A9})$$

Apparently, $G(r, r) = 0$.

For $\hat{G}_l(r, r')$, we have $L[r] = \hat{\mathcal{H}}_l$. One can take

$$f_1(r) = 1, \quad f_2(r) = \frac{K_{l+1}(mr)}{I_{l+1}(mr)}. \quad (\text{A10})$$

To see that $\hat{\mathcal{H}}_l f_2(r) = 0$, we recall that the operator $\hat{\mathcal{H}}_l$ is obtained via the following procedure

$$\widehat{\mathcal{M}}_l \psi_l = 0 \quad \Rightarrow \quad \hat{\mathcal{H}}_l \left(\frac{\psi_l}{\hat{\psi}_l} \right) = 0, \quad (\text{A11})$$

where $\hat{\psi}_l \sim r^{-1} I_{l+1}(mr)$ (cf. Eq. (37)) is a solution to $\widehat{\mathcal{M}}_l \psi_l = 0$. On the other hand, it is known that $\widehat{\mathcal{M}}_l \psi_l = 0$ has another solution regular at $r \rightarrow \infty, r^{-1} K_{l+1}(mr)$. One immediately sees that $\hat{\mathcal{H}}_l f_2(r) = 0$. With the basis solutions in Eq. (A10), we get Eq. (70).

For $G_l(r, r'; \varphi)$, we have $L[r] = \mathcal{H}[\varphi]$. In this case, to make the equation regular at $r \rightarrow \infty$ we can take

$$f_2(r) = g_2(r) \frac{K_{l+1}(mr)}{I_{l+1}(mr)}, \quad (\text{A12})$$

which gives

$$\frac{d^2 g_2(r)}{dr^2} - \left[2m \frac{K_l(mr)}{K_{l+1}(mr)} + \frac{2l+1}{r} \right] \frac{dg_2(r)}{dr} - W(\varphi(r)) g_2(r) = 0. \quad (\text{A13})$$

The boundary conditions are $g_2(r)|_{r \rightarrow \infty} \rightarrow 1, dg_2(r)/dr|_{r \rightarrow \infty} \rightarrow 0$.

⁹As a standard procedure for numerical calculations, one cannot take the boundary conditions strictly at $r = 0$, but instead at a value r_{\min} very close to zero. The boundary conditions at r_{\min} can be obtained via the Taylor expansion $f(r_{\min}) \approx f(0) + f'(0)r_{\min}$ and $f'(r_{\min}) = f'(0) + f''(0)r_{\min}$, where $f''(0)$ can be obtained by taking the limit $r \rightarrow 0$ for the equation to be solved. The infinity would be replaced by a large value r_{\max} depending on the numerical bounce solution.

A.2 $\mathcal{G}(r, r')$

According to the boundary condition for $\Delta\varphi_b$, one has the boundary condition for the Green's function

$$\mathcal{G}(r = \infty, r') = 0, \quad \left. \frac{\partial \mathcal{G}(r, r')}{\partial r} \right|_{r=0} = 0. \quad (\text{A14})$$

In this case, we can choose two independent solutions $\{f_1(r), f_2(r)\}$ satisfying, e.g.,

$$f_1(0) = 1, f_1'(r)|_{r=0} = 0; \quad f_2(r)|_{r \rightarrow \infty} \rightarrow 0, f_2'(r)|_{r \rightarrow \infty} \rightarrow 1. \quad (\text{A15})$$

A similar analysis gives

$$\mathcal{G}(r, r') = -\theta(r - r') \frac{f_1(r') f_2(r)}{\mathcal{W}[f_1(r'), f_2(r')]} - \theta(r' - r) \frac{f_2(r') f_1(r)}{\mathcal{W}[f_1(r'), f_2(r')]}, \quad (\text{A16})$$

Letting

$$f_1(r) = g_1(r) \frac{I_1(mr)}{r}, \quad f_2(r) = g_2(r) \frac{K_1(mr)}{r}, \quad (\text{A17})$$

we have

$$-g_1''(r) + \left[\frac{1}{r} - 2m \frac{I_0(mr)}{I_1(mr)} \right] g_1'(r) + W(\varphi_b^{(0)}(r)) g_1(r) = 0, \quad (\text{A18a})$$

$$-g_2''(r) + \left[\frac{1}{r} + 2m \frac{K_0(mr)}{K_1(mr)} \right] g_2'(r) + W(\varphi_b^{(0)}(r)) g_2(r) = 0, \quad (\text{A18b})$$

for which the boundary conditions can be chosen as, e.g., $g_1(0) = 2/m$, $g_1'(r)|_{r=0} = 0$ and $g_2(r)|_{r \rightarrow \infty} = 0$, $g_2'(r)|_{r \rightarrow \infty} = 1$. Note that $I_1(mr)/r \rightarrow m/2$ for $r \rightarrow 0$.

B Renormalisation with dimensional regularisation

In this appendix, we rederive the expression (46) of the regularized one-loop functional determinant originally presented in Ref. [47].

We start with Eq. (44). The divergent parts in ΔS are contained in $\Delta S^{(2)}$,

$$\Delta S^{(2)} = \frac{1}{2} \left[\ln \det(-\partial^2 + m^2 + W) - \ln \det(-\partial^2 + m^2) \right]_{\mathcal{O}(W^2)}, \quad (\text{B19})$$

so that we can write

$$S_1 = S_0^{\overline{\text{MS}}} + \underbrace{[\Delta S - \Delta S^{(2)}]}_{\text{numerical part}} + \underbrace{[\Delta S^{(2)} - (\Delta S)_{\text{pole}}]}_{\text{analytical part}}. \quad (\text{B20})$$

Our goal is to find two different expressions of $\Delta S^{(2)}$ such that the finite quantity $[\Delta S - \Delta S^{(2)}]$ can be computed numerically while the other finite quantity $[\Delta S^{(2)} - (\Delta S)_{\text{pole}}]$ can be computed analytically. For this purpose, we assign the perturbation W with a bookkeeping factor ε and expand $\ln \det(-\partial^2 + m^2 + \varepsilon W)$ in ε .

Numerically, we can write

$$\Delta S^{(2)} = \frac{1}{2} \sum_{l=0}^{\infty} (l+1)^2 \ln T_l(\infty; \varepsilon)|_{\mathcal{O}(\varepsilon^2)}. \quad (\text{B21})$$

where $T_l(\infty)$ is viewed as a function of ε and expanded in powers of ε ,

$$T_l(\infty; \varepsilon) = 1 + \varepsilon h_l^{(1)}(\infty) + \varepsilon^2 h_l^{(2)}(\infty) + \mathcal{O}(\varepsilon^3). \quad (\text{B22})$$

This gives

$$\ln T_l(\infty; \varepsilon)|_{\mathcal{O}(\varepsilon^2)} = h_l^{(1)}(\infty) + h_l^{(2)}(\infty) - \frac{1}{2}(h_l^{(1)}(\infty))^2. \quad (\text{B23})$$

To obtain $h_l^{(1)}(\infty)$ and $h_l^{(2)}(\infty)$, we substitute $T_l(r; \varepsilon) = 1 + \varepsilon h_l^{(1)}(r) + \varepsilon^2 h_l^{(2)}(r) + \mathcal{O}(\varepsilon^3)$ into Eq. (39)

$$\left[-\frac{d^2}{dr^2} - \left(2m \frac{I_{l+D/2-2}(mr)}{I_{l+D/2-1}(mr)} - \frac{2l+D-3}{r} \right) \frac{d}{dr} + \varepsilon W(\varphi(r)) \right] T_l(r; \varphi) = 0, \quad (\text{B24})$$

where the perturbation term is associated with a factor of ε now. Tracing the equations at the order of $\mathcal{O}(\varepsilon)$ and $\mathcal{O}(\varepsilon^2)$, we then obtain Eqs. (47) for $h_l^{(1)}(r)$ and $h_l^{(2)}(r)$.

To obtain the analytical part $[\Delta S^{(2)} - (\Delta S)_{\text{pole}}]$, we note that Eq. (B19) can be written as

$$\Delta S^{(2)} = \frac{1}{2} \text{Tr} [(-\partial^2 + m^2)^{-1} W] - \frac{1}{4} \text{Tr} [(-\partial^2 + m^2)^{-1} W (-\partial^2 + m^2) W]. \quad (\text{B25})$$

The first term is

$$\frac{1}{2} \int d^4x \langle x | (-\partial^2 + m^2)^{-1} W(\hat{x}) | x \rangle = \frac{1}{2} \left(\int \frac{d^4k}{(2\pi)^4} \frac{1}{k^2 + m^2} \right) \int d^4x W(x). \quad (\text{B26})$$

To do the $\overline{\text{MS}}$ regularization, we perform the momentum integral in d -dimensional spacetime, using the useful formula

$$\mu^{4-d} \int \frac{d^d k}{(2\pi)^d} \frac{1}{(k^2 + m^2)^\alpha} = \mu^{4-d} \frac{1}{(4\pi)^{d/2}} \frac{\Gamma(\alpha - \frac{d}{2})}{\Gamma(\alpha)} \frac{1}{m^{2\alpha-d}}. \quad (\text{B27})$$

Expanding the integral result around $d = 4$ (with $d = 4 - 2\epsilon$), one then obtains the pole. Subtracting the pole term according to the standard $\overline{\text{MS}}$ rule, one then obtains $A_{\text{fin}}^{(1)}$.

The second term on the RHS of Eq. (B25) can be written as

$$\begin{aligned}
& -\frac{1}{4} \int d^4x d^4y W(x)W(y) \int \frac{d^4q}{(2\pi)^4} e^{iq(x-y)} \left[\int \frac{d^4k}{(2\pi)^4} \frac{1}{(k+q)^2 + m^2} \frac{1}{k^2 + m^2} \right] \\
& = -\frac{1}{4} \int \frac{d^4q}{(2\pi)^4} \widetilde{W}(q) \widetilde{W}(-q) \times \left[\int \frac{d^4k}{(2\pi)^4} \frac{1}{(k+q)^2 + m^2} \frac{1}{k^2 + m^2} \right]. \tag{B28}
\end{aligned}$$

Again, the momentum integral inside the square brackets can be performed in d -dimensional spacetime by using the Feynman-parameter method, which in our case is

$$\frac{1}{AB} = \int_0^1 ds \frac{1}{sA + (1-s)B}. \tag{B29}$$

The final result of the momentum integral inside the square brackets is

$$\frac{1}{16\pi^2} \int_0^1 ds \left[\frac{1}{\epsilon} - \gamma_E + \ln 4\pi + \ln \frac{\mu^2}{s(1-s)q^2 + m^2} \right]. \tag{B30}$$

Finally, subtracting the pole term ($1/\epsilon$ together with $-\gamma_E + \ln 4\pi$) and doing the integral over s gives $A_{\text{fin}}^{(2)}$.

References

- [1] P. Q. Hung, “Vacuum Instability and New Constraints on Fermion Masses,” *Phys. Rev. Lett.* **42** (1979) 873.
- [2] M. Lindner, “Implications of Triviality for the Standard Model,” *Z. Phys. C* **31** (1986) 295.
- [3] M. Sher, “Electroweak Higgs Potentials and Vacuum Stability,” *Phys. Rept.* **179** (1989) 273–418.
- [4] M. Sher, “Precise vacuum stability bound in the standard model,” *Phys. Lett. B* **317** (1993) 159–163, [arXiv:hep-ph/9307342](#). [Addendum: *Phys.Lett.B* 331, 448–448 (1994)].
- [5] J. A. Casas, J. R. Espinosa, and M. Quiros, “Improved Higgs mass stability bound in the standard model and implications for supersymmetry,” *Phys. Lett. B* **342** (1995) 171–179, [arXiv:hep-ph/9409458](#).
- [6] J. A. Casas, J. R. Espinosa, and M. Quiros, “Standard model stability bounds for new physics within LHC reach,” *Phys. Lett. B* **382** (1996) 374–382, [arXiv:hep-ph/9603227](#).
- [7] G. Isidori, G. Ridolfi, and A. Strumia, “On the metastability of the standard model vacuum,” *Nucl. Phys. B* **609** (2001) 387–409, [arXiv:hep-ph/0104016](#).
- [8] C. P. Burgess, V. Di Clemente, and J. R. Espinosa, “Effective operators and vacuum instability as heralds of new physics,” *JHEP* **01** (2002) 041, [arXiv:hep-ph/0201160](#).

- [9] G. Isidori, V. S. Rychkov, A. Strumia, and N. Tetradis, “Gravitational corrections to standard model vacuum decay,” *Phys. Rev. D* **77** (2008) 025034, [arXiv:0712.0242 \[hep-ph\]](#).
- [10] J. Ellis, J. R. Espinosa, G. F. Giudice, A. Hoecker, and A. Riotto, “The Probable Fate of the Standard Model,” *Phys. Lett. B* **679** (2009) 369–375, [arXiv:0906.0954 \[hep-ph\]](#).
- [11] J. Elias-Miro, J. R. Espinosa, G. F. Giudice, G. Isidori, A. Riotto, and A. Strumia, “Higgs mass implications on the stability of the electroweak vacuum,” *Phys. Lett. B* **709** (2012) 222–228, [arXiv:1112.3022 \[hep-ph\]](#).
- [12] **ATLAS** Collaboration, G. Aad *et al.*, “Observation of a new particle in the search for the Standard Model Higgs boson with the ATLAS detector at the LHC,” *Phys. Lett. B* **716** (2012) 1–29, [arXiv:1207.7214 \[hep-ex\]](#).
- [13] **CMS** Collaboration, S. Chatrchyan *et al.*, “Observation of a New Boson at a Mass of 125 GeV with the CMS Experiment at the LHC,” *Phys. Lett. B* **716** (2012) 30–61, [arXiv:1207.7235 \[hep-ex\]](#).
- [14] **Tevatron Electroweak Working Group, CDF, D0** Collaboration, “Combination of CDF and D0 results on the mass of the top quark using up to 5.8[~]fb⁻¹ of data,” [arXiv:1107.5255 \[hep-ex\]](#).
- [15] G. Degrandi, S. Di Vita, J. Elias-Miro, J. R. Espinosa, G. F. Giudice, G. Isidori, and A. Strumia, “Higgs mass and vacuum stability in the Standard Model at NNLO,” *JHEP* **08** (2012) 098, [arXiv:1205.6497 \[hep-ph\]](#).
- [16] D. Buttazzo, G. Degrandi, P. P. Giardino, G. F. Giudice, F. Sala, A. Salvio, and A. Strumia, “Investigating the near-criticality of the Higgs boson,” *JHEP* **12** (2013) 089, [arXiv:1307.3536 \[hep-ph\]](#).
- [17] L. Di Luzio, G. Isidori, and G. Ridolfi, “Stability of the electroweak ground state in the Standard Model and its extensions,” *Phys. Lett. B* **753** (2016) 150–160, [arXiv:1509.05028 \[hep-ph\]](#).
- [18] S. Chigusa, T. Moroi, and Y. Shoji, “State-of-the-Art Calculation of the Decay Rate of Electroweak Vacuum in the Standard Model,” *Phys. Rev. Lett.* **119** no. 21, (2017) 211801, [arXiv:1707.09301 \[hep-ph\]](#).
- [19] A. Andreassen, W. Frost, and M. D. Schwartz, “Scale Invariant Instantons and the Complete Lifetime of the Standard Model,” *Phys. Rev. D* **97** no. 5, (2018) 056006, [arXiv:1707.08124 \[hep-ph\]](#).
- [20] S. R. Coleman, “The Fate of the False Vacuum. 1. Semiclassical Theory,” *Phys. Rev. D* **15** (1977) 2929–2936. [Erratum: *Phys.Rev.D* 16, 1248 (1977)].
- [21] C. G. Callan, Jr. and S. R. Coleman, “The Fate of the False Vacuum. 2. First Quantum Corrections,” *Phys. Rev. D* **16** (1977) 1762–1768.
- [22] B. Garbrecht and P. Millington, “Green’s function method for handling radiative effects on false vacuum decay,” *Phys. Rev. D* **91** (2015) 105021, [arXiv:1501.07466 \[hep-th\]](#).

- [23] M. A. Bezuglov and A. I. Onishchenko, “Two-loop corrections to false vacuum decay in scalar field theory,” *Phys. Lett. B* **788** (2019) 122–130, [arXiv:1805.06482 \[hep-ph\]](#).
- [24] M. A. Bezuglov and A. I. Onishchenko, “NNLO corrections to false vacuum decay rate in thin-wall approximation,” [arXiv:1903.10864 \[hep-ph\]](#).
- [25] W.-Y. Ai, B. Garbrecht, and P. Millington, “Radiative effects on false vacuum decay in Higgs-Yukawa theory,” *Phys. Rev. D* **98** no. 7, (2018) 076014, [arXiv:1807.03338 \[hep-th\]](#).
- [26] W.-Y. Ai, J. S. Cruz, B. Garbrecht, and C. Tamarit, “Gradient effects on false vacuum decay in gauge theory,” *Phys. Rev. D* **102** no. 8, (2020) 085001, [arXiv:2006.04886 \[hep-th\]](#).
- [27] J. Baacke and N. Kevlishvili, “False vacuum decay by self-consistent bounces in four dimensions,” *Phys. Rev. D* **75** (2007) 045001, [arXiv:hep-th/0611004](#). [Erratum: *Phys.Rev.D* 76, 029903 (2007)].
- [28] Y. Bergner and L. M. A. Bettencourt, “Dressing up the kink,” *Phys. Rev. D* **69** (2004) 045002, [arXiv:hep-th/0305190](#).
- [29] Y. Bergner and L. M. A. Bettencourt, “The Selfconsistent bounce: An Improved nucleation rate,” *Phys. Rev. D* **69** (2004) 045012, [arXiv:hep-ph/0308107](#).
- [30] J. Baacke and N. Kevlishvili, “Self-consistent bounces in two dimensions,” *Phys. Rev. D* **71** (2005) 025008, [arXiv:hep-th/0411162](#).
- [31] I. M. Gelfand and A. M. Yaglom, “Integration in functional spaces and it applications in quantum physics,” *J. Math. Phys.* **1** (1960) 48.
- [32] W.-Y. Ai, B. Garbrecht, and C. Tamarit, “Functional methods for false vacuum decay in real time,” *JHEP* **12** (2019) 095, [arXiv:1905.04236 \[hep-th\]](#).
- [33] R. Jackiw, “Functional evaluation of the effective potential,” *Phys. Rev. D* **9** (1974) 1686.
- [34] A. D. Plascencia and C. Tamarit, “Convexity, gauge-dependence and tunneling rates,” *JHEP* **10** (2016) 099, [arXiv:1510.07613 \[hep-ph\]](#).
- [35] W.-Y. Ai and M. Drewes, “Schwinger effect and false vacuum decay as quantum-mechanical tunneling of a relativistic particle,” *Phys. Rev. D* **102** no. 7, (2020) 076015, [arXiv:2005.14163 \[hep-th\]](#).
- [36] J.-L. Gervais and B. Sakita, “Extended Particles in Quantum Field Theories,” *Phys. Rev. D* **11** (1975) 2943.
- [37] B. Garbrecht and P. Millington, “Constraining the effective action by a method of external sources,” *Nucl. Phys. B* **906** (2016) 105–132, [arXiv:1509.07847 \[hep-th\]](#).
- [38] B. Garbrecht and P. Millington, “Self-consistent solitons for vacuum decay in radiatively generated potentials,” *Phys. Rev. D* **92** (2015) 125022, [arXiv:1509.08480 \[hep-ph\]](#).
- [39] J. M. Cornwall, R. Jackiw, and E. Tomboulis, “Effective Action for Composite Operators,” *Phys. Rev. D* **10** (1974) 2428–2445.

- [40] G. V. Dunne and H. Min, “Beyond the thin-wall approximation: Precise numerical computation of prefactors in false vacuum decay,” *Phys. Rev. D* **72** (2005) 125004, [arXiv:hep-th/0511156](#).
- [41] V. Guada and M. Nemevšek, “Exact one-loop false vacuum decay rate,” *Phys. Rev. D* **102** (2020) 125017, [arXiv:2009.01535 \[hep-th\]](#).
- [42] A. Ivanov, A. Ivanov, M. Matteini, M. Matteini, M. Nemevšek, M. Nemevšek, L. Ubaldi, and L. Ubaldi, “Analytic thin wall false vacuum decay rate,” *JHEP* **03** (2022) 209, [arXiv:2202.04498 \[hep-th\]](#). [Erratum: JHEP 07, 085 (2022), Erratum: JHEP 11, 157 (2022)].
- [43] A. Ekstedt, O. Gould, and J. Hirvonen, “BubbleDet: a Python package to compute functional determinants for bubble nucleation,” *JHEP* **12** (2023) 056, [arXiv:2308.15652 \[hep-ph\]](#).
- [44] G. V. Dunne and K. Kirsten, “Functional determinants for radial operators,” *J. Phys. A* **39** (2006) 11915–11928, [arXiv:hep-th/0607066](#).
- [45] G. V. Dunne, “Functional determinants in quantum field theory,” *J. Phys. A* **41** (2008) 304006, [arXiv:0711.1178 \[hep-th\]](#).
- [46] J. Baacke and V. G. Kiselev, “One loop corrections to the bubble nucleation rate at finite temperature,” *Phys. Rev. D* **48** (1993) 5648–5654, [arXiv:hep-ph/9308273](#).
- [47] J. Baacke and G. Lavrelashvili, “One loop corrections to the metastable vacuum decay,” *Phys. Rev. D* **69** (2004) 025009, [arXiv:hep-th/0307202](#).
- [48] V. Branchina, E. Messina, and M. Sher, “Lifetime of the electroweak vacuum and sensitivity to Planck scale physics,” *Phys. Rev. D* **91** (2015) 013003, [arXiv:1408.5302 \[hep-ph\]](#).
- [49] A. Andreassen, D. Farhi, W. Frost, and M. D. Schwartz, “Precision decay rate calculations in quantum field theory,” *Phys. Rev. D* **95** no. 8, (2017) 085011, [arXiv:1604.06090 \[hep-th\]](#).
- [50] J. R. Espinosa, “A Fresh Look at the Calculation of Tunneling Actions,” *JCAP* **07** (2018) 036, [arXiv:1805.03680 \[hep-th\]](#).
- [51] J. Braden, M. C. Johnson, H. V. Peiris, A. Pontzen, and S. Weinfurtner, “New Semiclassical Picture of Vacuum Decay,” *Phys. Rev. Lett.* **123** no. 3, (2019) 031601, [arXiv:1806.06069 \[hep-th\]](#). [Erratum: Phys.Rev.Lett. 129, 059901 (2022)].
- [52] J. R. Espinosa, “Fresh look at the calculation of tunneling actions including gravitational effects,” *Phys. Rev. D* **100** no. 10, (2019) 104007, [arXiv:1808.00420 \[hep-th\]](#).
- [53] J. R. Espinosa and T. Konstandin, “A Fresh Look at the Calculation of Tunneling Actions in Multi-Field Potentials,” *JCAP* **01** (2019) 051, [arXiv:1811.09185 \[hep-th\]](#).
- [54] W.-Y. Ai, “Correspondence between Thermal and Quantum Vacuum Transitions around Horizons,” *JHEP* **03** (2019) 164, [arXiv:1812.06962 \[hep-th\]](#).

- [55] M. P. Hertzberg and M. Yamada, “Vacuum Decay in Real Time and Imaginary Time Formalisms,” *Phys. Rev. D* **100** no. 1, (2019) 016011, [arXiv:1904.08565 \[hep-th\]](#).
- [56] S. Chigusa, T. Moroi, and Y. Shoji, “Bounce Configuration from Gradient Flow,” *Phys. Lett. B* **800** (2020) 135115, [arXiv:1906.10829 \[hep-ph\]](#).
- [57] J. R. Espinosa, “Tunneling without Bounce,” *Phys. Rev. D* **100** no. 10, (2019) 105002, [arXiv:1908.01730 \[hep-th\]](#).
- [58] L. Darmé, J. Jaeckel, and M. Lewicki, “Generalized escape paths for dynamical tunneling in QFT,” *Phys. Rev. D* **100** no. 9, (2019) 096012, [arXiv:1907.04865 \[hep-th\]](#).
- [59] Z.-G. Mou, P. M. Saffin, and A. Tranberg, “Quantum tunnelling, real-time dynamics and Picard-Lefschetz thimbles,” *JHEP* **11** (2019) 135, [arXiv:1909.02488 \[hep-th\]](#).
- [60] D. Croon, E. Hall, and H. Murayama, “Non-perturbative methods for false vacuum decay,” [arXiv:2104.10687 \[hep-th\]](#).
- [61] T. Hayashi, K. Kamada, N. Oshita, and J. Yokoyama, “Vacuum decay in the Lorentzian path integral,” *JCAP* **05** no. 05, (2022) 041, [arXiv:2112.09284 \[hep-th\]](#).
- [62] P. Draper, M. Karydas, and H. Zhang, “Vacuum decay in time-dependent backgrounds,” *Phys. Rev. D* **108** no. 9, (2023) 096038, [arXiv:2306.01609 \[hep-th\]](#).
- [63] J. Nishimura, K. Sakai, and A. Yosprakob, “A new picture of quantum tunneling in the real-time path integral from Lefschetz thimble calculations,” *JHEP* **09** (2023) 110, [arXiv:2307.11199 \[hep-th\]](#).
- [64] K. Blum and O. Rosner, “Unraveling the bounce: a real time perspective on tunneling,” [arXiv:2309.07585 \[quant-ph\]](#).
- [65] L. Batini, A. Chatrchyan, and J. Berges, “Real-time dynamics of false vacuum decay,” *Phys. Rev. D* **109** no. 2, (2024) 023502, [arXiv:2310.04206 \[hep-th\]](#).
- [66] T. Steingasser, M. König, and D. I. Kaiser, “Finite-Temperature Instantons from First Principles,” [arXiv:2310.19865 \[hep-th\]](#).
- [67] D. Pîrvu, M. C. Johnson, and S. Sibiryakov, “Bubble velocities and oscillon precursors in first order phase transitions,” [arXiv:2312.13364 \[hep-th\]](#).
- [68] J. Baacke and S. Junker, “Quantum corrections to the electroweak sphaleron transition,” *Mod. Phys. Lett. A* **8** (1993) 2869–2874, [arXiv:hep-ph/9306307](#).
- [69] J. Baacke and S. Junker, “Quantum fluctuations around the electroweak sphaleron,” *Phys. Rev. D* **49** (1994) 2055–2073, [arXiv:hep-ph/9308310](#).
- [70] J. Baacke and S. Junker, “Quantum fluctuations of the electroweak sphaleron: Erratum and addendum,” *Phys. Rev. D* **50** (1994) 4227–4228, [arXiv:hep-th/9402078](#).
- [71] J. Baacke, “One-loop corrections to the instanton transition in the Abelian Higgs model: Gel’fand-Yaglom and Green’s function methods,” *Phys. Rev. D* **78** (2008) 065039, [arXiv:0803.4333 \[hep-th\]](#).

- [72] N. K. Nielsen, “On the Gauge Dependence of Spontaneous Symmetry Breaking in Gauge Theories,” *Nucl. Phys. B* **101** (1975) 173–188.
- [73] R. Fukuda and T. Kugo, “Gauge Invariance in the Effective Action and Potential,” *Phys. Rev. D* **13** (1976) 3469.
- [74] D. Metaxas and E. J. Weinberg, “Gauge independence of the bubble nucleation rate in theories with radiative symmetry breaking,” *Phys. Rev. D* **53** (1996) 836–843, [arXiv:hep-ph/9507381](#).
- [75] M. Garny and T. Konstandin, “On the gauge dependence of vacuum transitions at finite temperature,” *JHEP* **07** (2012) 189, [arXiv:1205.3392 \[hep-ph\]](#).
- [76] M. Endo, T. Moroi, M. M. Nojiri, and Y. Shoji, “On the Gauge Invariance of the Decay Rate of False Vacuum,” *Phys. Lett. B* **771** (2017) 281–287, [arXiv:1703.09304 \[hep-ph\]](#).
- [77] M. Endo, T. Moroi, M. M. Nojiri, and Y. Shoji, “False Vacuum Decay in Gauge Theory,” *JHEP* **11** (2017) 074, [arXiv:1704.03492 \[hep-ph\]](#).
- [78] O. Gould and J. Hirvonen, “Effective field theory approach to thermal bubble nucleation,” *Phys. Rev. D* **104** no. 9, (2021) 096015, [arXiv:2108.04377 \[hep-ph\]](#).
- [79] J. Löfgren, M. J. Ramsey-Musolf, P. Schicho, and T. V. I. Tenkanen, “Nucleation at Finite Temperature: A Gauge-Invariant Perturbative Framework,” *Phys. Rev. Lett.* **130** no. 25, (2023) 251801, [arXiv:2112.05472 \[hep-ph\]](#).
- [80] J. Hirvonen, J. Löfgren, M. J. Ramsey-Musolf, P. Schicho, and T. V. I. Tenkanen, “Computing the gauge-invariant bubble nucleation rate in finite temperature effective field theory,” *JHEP* **07** (2022) 135, [arXiv:2112.08912 \[hep-ph\]](#).
- [81] D. E. Morrissey and M. J. Ramsey-Musolf, “Electroweak baryogenesis,” *New J. Phys.* **14** (2012) 125003, [arXiv:1206.2942 \[hep-ph\]](#).
- [82] P. Athron, C. Balázs, A. Fowlie, L. Morris, and L. Wu, “Cosmological phase transitions: From perturbative particle physics to gravitational waves,” *Prog. Part. Nucl. Phys.* **135** (2024) 104094, [arXiv:2305.02357 \[hep-ph\]](#).
- [83] D. Croon, “TASI lectures on Phase Transitions, Baryogenesis, and Gravitational Waves,” *PoS TASI2022* (2024) 003, [arXiv:2307.00068 \[hep-ph\]](#).
- [84] J. S. Langer, “Theory of the condensation point,” *Annals Phys.* **41** (1967) 108–157.
- [85] J. S. Langer, “Statistical theory of the decay of metastable states,” *Annals Phys.* **54** (1969) 258–275.
- [86] I. Affleck, “Quantum Statistical Metastability,” *Phys. Rev. Lett.* **46** (1981) 388.
- [87] A. D. Linde, “Fate of the False Vacuum at Finite Temperature: Theory and Applications,” *Phys. Lett. B* **100** (1981) 37–40.
- [88] A. D. Linde, “Decay of the False Vacuum at Finite Temperature,” *Nucl. Phys. B* **216** (1983) 421. [Erratum: *Nucl.Phys.B* 223, 544 (1983)].

- [89] S. R. Coleman and F. De Luccia, “Gravitational Effects on and of Vacuum Decay,” *Phys. Rev. D* **21** (1980) 3305.
- [90] R. Gregory, I. G. Moss, and B. Withers, “Black holes as bubble nucleation sites,” *JHEP* **03** (2014) 081, [arXiv:1401.0017 \[hep-th\]](#).
- [91] D. Canko, I. Gialamas, G. Jelic-Cizmek, A. Riotto, and N. Tetradis, “On the Catalysis of the Electroweak Vacuum Decay by Black Holes at High Temperature,” *Eur. Phys. J. C* **78** no. 4, (2018) 328, [arXiv:1706.01364 \[hep-th\]](#).
- [92] K. Mukaida and M. Yamada, “False Vacuum Decay Catalyzed by Black Holes,” *Phys. Rev. D* **96** no. 10, (2017) 103514, [arXiv:1706.04523 \[hep-th\]](#).
- [93] T. Hayashi, K. Kamada, N. Oshita, and J. Yokoyama, “On catalyzed vacuum decay around a radiating black hole and the crisis of the electroweak vacuum,” *JHEP* **08** (2020) 088, [arXiv:2005.12808 \[hep-th\]](#).
- [94] A. Shkerin and S. Sibiryakov, “Black hole induced false vacuum decay from first principles,” *JHEP* **11** (2021) 197, [arXiv:2105.09331 \[hep-th\]](#).
- [95] A. Shkerin and S. Sibiryakov, “Black hole induced false vacuum decay: the role of greybody factors,” *JHEP* **08** (2022) 161, [arXiv:2111.08017 \[hep-th\]](#).
- [96] R. Gregory and S.-Q. Hu, “Seeded vacuum decay with Gauss-Bonnet,” *JHEP* **11** (2023) 072, [arXiv:2305.03006 \[hep-th\]](#).
- [97] P. Hanggi, P. Talkner, and M. Borkovec, “Reaction-Rate Theory: Fifty Years After Kramers,” *Rev. Mod. Phys.* **62** (1990) 251–341.
- [98] A. Berera, J. Mabillard, B. W. Mintz, and R. O. Ramos, “Formulating the Kramers problem in field theory,” *Phys. Rev. D* **100** no. 7, (2019) 076005, [arXiv:1906.08684 \[hep-ph\]](#).
- [99] A. Ekstedt, “Higher-order corrections to the bubble-nucleation rate at finite temperature,” *Eur. Phys. J. C* **82** no. 2, (2022) 173, [arXiv:2104.11804 \[hep-ph\]](#).
- [100] D. Croon, O. Gould, P. Schicho, T. V. I. Tenkanen, and G. White, “Theoretical uncertainties for cosmological first-order phase transitions,” *JHEP* **04** (2021) 055, [arXiv:2009.10080 \[hep-ph\]](#).
- [101] H.-K. Guo, K. Sinha, D. Vagie, and G. White, “The benefits of diligence: how precise are predicted gravitational wave spectra in models with phase transitions?,” *JHEP* **06** (2021) 164, [arXiv:2103.06933 \[hep-ph\]](#).
- [102] J. Braden, M. C. Johnson, H. V. Peiris, and S. Weinfurtner, “Towards the cold atom analog false vacuum,” *JHEP* **07** (2018) 014, [arXiv:1712.02356 \[hep-th\]](#).
- [103] J. Braden, M. C. Johnson, H. V. Peiris, A. Pontzen, and S. Weinfurtner, “Nonlinear Dynamics of the Cold Atom Analog False Vacuum,” *JHEP* **10** (2019) 174, [arXiv:1904.07873 \[hep-th\]](#).
- [104] A. C. Jenkins, J. Braden, H. V. Peiris, A. Pontzen, M. C. Johnson, and S. Weinfurtner,

- “Analog vacuum decay from vacuum initial conditions,” *Phys. Rev. D* **109** no. 2, (2024) 023506, [arXiv:2307.02549 \[cond-mat.quant-gas\]](#).
- [105] A. Zenesini, A. Berti, R. Cominotti, C. Rogora, I. G. Moss, T. P. Billam, I. Carusotto, G. Lamporesi, A. Recati, and G. Ferrari, “Observation of false vacuum decay via bubble formation in ferromagnetic superfluids,” [arXiv:2305.05225 \[hep-ph\]](#).